Accession No. _____

Contract Program or Project Title: Thermal Fuels Behavior Program

Subject of this Document: "PBF/LOFT Lead Rod Program Test LLR-4A Quick Look Report"
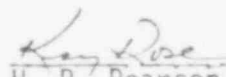
Type of Document: Quick Look Report

Author(s):   D. J. Varacalle, Jr., R. W. Garner

Date of Document: June 1979

Responsible NRC Individual and NRC Office or Division: G. D. McPherson

This document was prepared primarily for preliminary or internal use. It has not received full review and approval. Since there may be substantive changes, this document should not be considered final.

H. P. Pearson, Supervisor
Information Processing
EG&G Idaho, Inc.

INTERIM REPORT

480   129

7908020474

PBF/LOFT LEAD ROD PROGRAM
TEST LLR-4A QUICK LOOK REPORT

D.J. VARACALLE, JR.   R.W. GARNER

June 1979

NRC Research and Technical
Assistance Report

EG&G Idaho, Inc.

IDAHO NATIONAL ENGINEERING LABORATORY

DEPARTMENT OF ENERGY

480   130

PBF/LOFT LEAD ROD PROGRAM
TEST LLR-4A
QUICK LOOK REPORT

June 1979

D. J. Varacalle, Jr.
R. W. Garner

Approved:

_____

R. W. Garner, Supervisor
PBF/LOFT Lead Rod Test Section

_____

R. K. McCardell, Manager
PBF Experiment Specification and
Analysis Branch

_____

P. E. McDonald, Manager
LWR Fuel Research Division

Thermal Fuels Behavior Program
EG&G Idaho, Inc.

480 131

INTERIM REPORT

Accession No

Report No. TFBP-TR-320

Contract Program or Project Title:

Thermal Fuels Behavior Program

Subject of this Document:

PBF/LOFT Lead Rod Program Test LLR-4A Quick Look Report

Type of Document:

QLR

Author(s):

D. J. Varacalle, Jr., R. W. Garner

Date of Document:

June, 1979

Responsible NRC Individual and NRC Office or Division:

G. D. McPherson

EG&G Idaho, Inc.
Idaho Falls, Idaho 83401

INTERIM REPORT

480 132

NRC Research and Technical
Assistance Report

SUMMARY

This report describes the preliminary results of the PBF/LOFT
Lead Rod (LLR) Program Test LLR-4A conducted in the Power Burst
Facility Test Reactor at the Idaho National Engineering Laboratory.
Test LLR-4A was conducted on May 18, 1979. The PBF/LLR Tests (LLR-3,
LLR-5, and LLR-4) were designed to simulate the test conditions for
LOFT loss-of-coolant experiment (LOCEs) tests L2-3 through L2-5. Test
LLR-4A was added to the PBF/LLR program following completion of Test
LLR-4 to investigate the effects of preconditioning and a successive
LOCE transient on deformed fuel rods. The test conditions and
performance sequence for this test were identical to the LLR-4 test.

Four separately shrouded PWR-type fuel rods were utilized for the
LLR-4A test. A total of seven fuel rods were tested in the PBF
in-pile tube (IPT) during the four LLR tests. The LLR-4A rods were
designated as 399-2, 312-2, 345-1, and 345-2. The fuel rods consisted
of a 0.914 m long fuel stack of fresh, 93% theoretical density,
9.5 wt% UO_2 fuel, and were backfilled with helium at atmospheric
pressure (0.10 MPa). Rod 312-2 had been used in Tests LLR-3, LLR-5,
and LLR-4; Rods 345-1 and 345-2 had been used in Tests LLR-5 and
LLR-4; and Rod 399-2 was a fresh rod, installed for Test LLR-4A.

The LLR-4A test consisted of a power calibration phase, a decay
heat buildup phase, a blowdown phase, and reflood and quench cooling
phases. During the test, blowdown was initiated at coolant conditions
of approximately 600 K IPT inlet coolant temperature, a coolant
flowrate of 0.78 1/s per flow shroud, a system pressure of 15.5 MPa,
and rod peak power densities of 56 kW/m. The rods were subjected to a
blowdown similar to that to be expected in LOFT during a 200%
double-ended cold leg break, followed by reflood and quench cooling.

Maximum cladding temperatures attained during Test LLR-4A were:
rod 399-2, 1260 K; rod 312-2, 1150 K and rod 345-1, 1075 K. Rod 345-2
was not instrumented with cladding thermocouples. Based on these

temperatures it is expected that rods 399-2 and 312-2 reached the waisting regime of mechanical deformation, while rod 345-1 reached the collapse regime.

CONTENTS

FIGURES

TABLES

480 137

vi

1. INTRODUCTION

Understanding the behavior of light-water reactor (LWR) fuels
under loss-of-coolant accident conditions is a major objective of the
Nuclear Regulatory Commission's (NRC) Reactor Safety Research
Program. The Loss of Fluid Test (LOFT) facility is the major NRC
sponsored testing facility to simulate the response of an LWR over a
wide range of loss of coolant accident conditions. As such, the LOFT
core is intended to be used for sequential Loss-of-Coolant Experiment
(LOCE) tests, provided extensive fuel rod failures do not occur.

A series of tests has been performed in the Power Burst Facility
at the Idaho National Engineering Laboratory for the purpose of
providing a parametric evaluation of the expected mechanical response
of the LOFT fuel rods to a loss of coolant from a wide range of
initial power levels. These tests are called the PBF/LOFT Lead Rod
(LLR) Tests. The specific objectives of the PBF/LLR Tests are:
(a) to experimentally evaluate the extent of cladding collapse that
would be expected to occur during the LOFT LOCA transients, (b) to
evaluate the effects of collapsed cladding and pellet-cladding
interaction (PCI) on the mechanical response of the fuel rods
subjected to subsequent power increases, long term preconditioning,
and loss-of-coolant conditions, and (c) to provide experimental data
to benchmark the Fuel Rod Analysis Program (FRAP) that will be used
for requalification of the LOFT core. The PBF/LLR Test Program has
consisted of four tests: LLR-3, LLR-5, and LLR-4, corresponding to
the planned LOFT L2-3, L2-5, and L2-4 tests, respectively, and Test
LLR-4A, a follow-on test to the original program. Each of the LLR
tests was performed with four identical, separately shrouded LOFT
design fuel rods with an active length of 0.914 m. Each test
consisted of six phases of operation: (a) system heatup, (b) nuclear
power calibration, (c) steady state operation to precondition the fuel
and to build up a fission product inventory, (d) system blowdown,
(e) system reflood, and (f) quench and cooldown.

1

During Test LLR-4A, the power calibration phase consisted of operating at several power levels to provide fuel preconditioning and intercalibration of the test rods with the PBF core power. The rods were then further preconditioned at a test rod peak power density of 56 kW/m. Preconditioning lasted for approximately 3 hours for the test and provided 82% decay heat buildup. System conditions prior to blowdown were approximately: 600 K inlet coolant temperature, coolant flowrate through each flow shroud of 0.78 l/s, and system pressure of 15.5 MPa. Upon completion of the preconditioning phase for the test, blowdown was initiated by opening the high speed valves in the cold leg, simulating a 200% double-ended cold leg break.

For Test LLR-4A, all of the rods were surrounded by zircaloy shrouds. Consequently, all four rods experienced the same power conditions.

The following sections provide brief descriptions of the PBF/LLR experiment design and test conduct, and preliminary test results for Test LLR-4A.

480   139

2. EXPERIMENT DESIGN

The PBF/LLR Tests were performed with four identical, separately shrouded PWR type fuel rods. The fuel rods, individual flow shrouds, and instrumentation were supported by the test train. This section briefly describes the design of the fuel rods, flow shrouds, test train, reflood system, and Loss of Coolant Accident (LOCA) Blowdown System; and lists the instrumentation associated with each component. Further information is available in the Experiment Specification Document (ESD)[1], the Experiment Configuration Specification (ECS)[2], and the Experiment Operating Specification (EOS)[3].

2.1 Fuel Rods

The geometry of the active length of the fuel rods is identical with a LOFT fuel rod. LOFT cladding was utilized to fabricate the fuel rods. The plenum pressure selected corresponds to the backfill pressure utilized for the LOFT L2 Test series fuel rods (.1034 MPa, 15 psia). The fuel rod designations for each test, and cladding surface thermocouple locations for each rod are shown in Table I. The fuel rod design characteristics are listed in Table II. As shown in Table I, Rods 312-2, 345-1, 345-2, and 399-2 were used in Test LLR-4A. Rod 312-2 had also been used in Tests LLR-3, LLR-5, and LLR-4. Rods 345-1, and 345-2 had also been used in Test LLR-5 and LLR-4, and Rod 399-2 was a fresh rod incorporated for Test LLR-4A.

2.2 Flow Shrouds

Each fuel rod was encased within a flow shroud as part of the fuel train, which also included the associated instrumentation discussed in Section 2.5. Circular flow shrouds, as shown in Figure 1, were utilized for the entire test series. For the LLR-4A test all the rods were encased in Zircaloy-4 flow shrouds.

480   140

TABLE I

FUEL ROD DESIGNATIONS AND CLADDING SURFACE THERMOCOUPLE LOCATIONS FOR PBF/LOFT LEAD ROD TESTS

				*Thermocouple Location (m)			
Rod	Number	Tests LLR-	Shroud	Clad T/C #1 180° Orientation	Clad T/C #2 0° Orientation	Centerline T/C	**
1	312-1	3,4,5	Zirc	0.533	0.533	0.533	yes
2	312-2	3,4,5,4A	Zirc	0.533	0.457	0.457	no
3	312-3	3	SS	0.533	0.533	0.533	yes
4	312-4	3	SS	0.533	0.533	0.533	no
5	345-1	4,5,4A	Zirc	0.533	0.533	0.533	yes
6	345-2	4,5,4A	Zirc	-	-	0.457	no
7	399-1	Spare	Zirc	0.533	0.457	0.457	no
8	399-2	4A	Zirc	0.457	0.314	0.457	yes

* From bottom of active fuel.
   All rods were unpressurized (0.1034 MPa, 15 psia).

** Instrumented with 3 bulk coolant thermocouples and 3 flow shroud
   thermocouples at fuel midplane and 120 mm above and below the midplane.

480 141

4

TABLE II

PBF/LOFT LEAD ROD TEST FUEL ROD DESIGN CHARACTERISTICS

Characteristics	Nominal Value

Fuel

Material	UO_2, (References 4 & 5)
Pellet OD	0.9294 + 0.00127 cm
	(0.3659 + 0.0005 in.)
Pellet length	1.524 + .0635 cm
	(0.600 + 0.025 in.)
Pellet enrichment	9.5 + 0.5 WT%
Density	93.0 + 1.5% TD
Fuel stack length	0.9144 m (36.0 in. + 0.03)
End configuration	Dished
Burnup	0 MWd/t
Centerhole diameter	0.185 cm (0.073 in. + 0.002)

Insulator Pellet

Material	Al_2O_3 (99% pure, ASTM D2442)
Length	0.508 + 0.0254 cm (0.2 + 0.010 in.)
Diameter	0.889 + .005 cm (0.35 + 0.002 in.)

Cladding

Material	Zircaloy-4 (Reference 6)
Tube OD	1.07 + 0.0038 cm (0.424 + 0.0015 in)
Tube ID	0.948 + 0.0038 cm (0.3734 + 0.0015 in.)
Thickness	0.061 cm (0.0243 in.) nominal
Yield strength	(Reference 6)
Ultimate strength	(Reference 6)
Maximum bow	(Reference 6)
Overall length	99.06 cm

Fuel Rod

Plenum void volume	2.95 cm^3 (0.18 $in.^3$ + 5%)
Filler gas	He
Filler gas purity	94.9% He, 5% Ar, 0.1% impurities
Initial gas pressure	0.1034 MPa (15 psia)
Diametral gap	0.0191 cm (0.0075 in.)
Overall length	99.8601 cm

6

Test Configuration Schematic

Internal pressure transducer and thermocouple

Coolant thermocouple

Flow shroud

Cladding surface thermocouples

Fuel rod

Centerline thermocouple

Bypass flow region

Coolant flow path

INEL-S-15 759

Bottom of the fuel rod

LVDT

480 143

Turbine flowmeter

Inlet thermocouples

Inlet flow
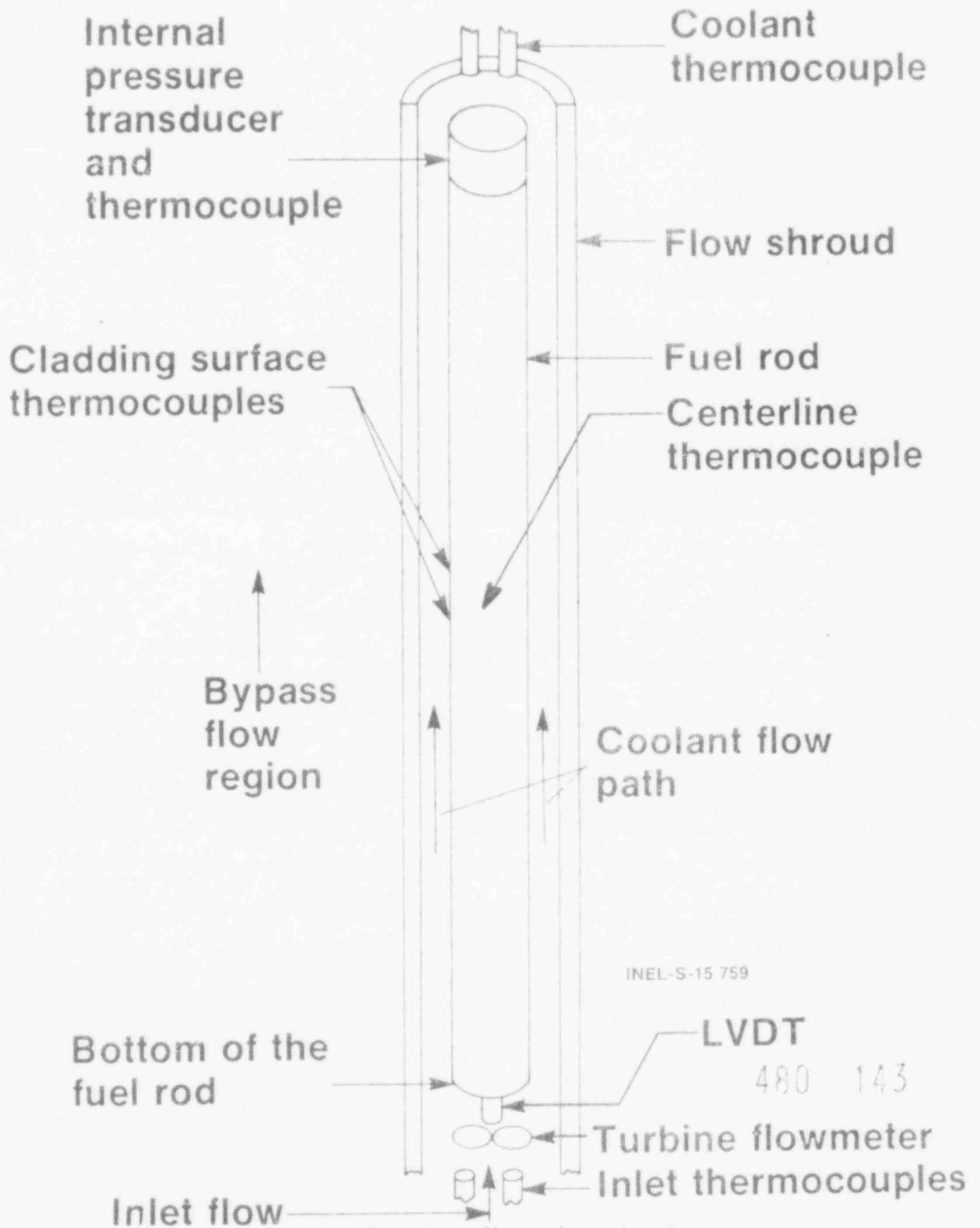
Fig. 1 PBF/LLR test configuration schematic.

2.3 Test Train

Figure 2 presents an illustration of the PBF/LLR test train installed in the PBF IPT. During pre-blowdown steady state conditions, the coolant enters the PBF reactor In-Pile Tube (IPT) where approximately 75% of the coolant flows upwards through a controlled bypass flow path from the IPT cold leg inlet to the upper plenum, and the remaining coolant passes downward outside the IPT flow shroud to the vicinity of the catch basket. The IPT flow shroud is stainless steel except along the region of the active fuel rod, where it is Zircaloy-4.

The coolant that flows downward to the catch basket then enters each of the four test rod flow shrouds. The lower fuel rod support plate is designed to minimize bypass flow past the fuel rod shrouds to less than 2% of the total experiment core flow.

The coolant then passes inside each circular flow shroud, past each fuel rod, and out an exit tube to the common upper plenum region. The total IPT flow then passes through the upper particle screen where it mixes with the controlled bypass flow and then exits.

To provide relative water volumes in the test rod region and other volumes in the system characteristic of the LOFT system, filler pieces were inserted in the IPT exit volume, the upper plenum, and the downcomer region, as shown in Figure 2.

A central hanger rod (28.57 mm OD, 15.88 mm ID) was used in the 4X hardware design to support the test train. The hanger rod is zircaloy tubing in the active core region. The capability for reflood water was provided through this tube, with a direct injection, constant flow rate reflood system.

A controlled bypass flow path between the IPT inlet and the upper plenum was provided across the IPT flow tube. The bypass consists of a single hole sized for approximately 75% of the total IPT flow at

7

(Not to scale)

IPT upper head

Filter pieces

Inpile tube

Outlet

Upper plenum

Inlet

Controlled bypass

Upper particle screen

Center hanger rod

Check valve

Flow tube

Fuel rod and flow shroud

Bypass volume

Downcomer filler piece

Lower support plate

Lower particle screen

Catch basket

Lower plenum

INEL-A-10 142
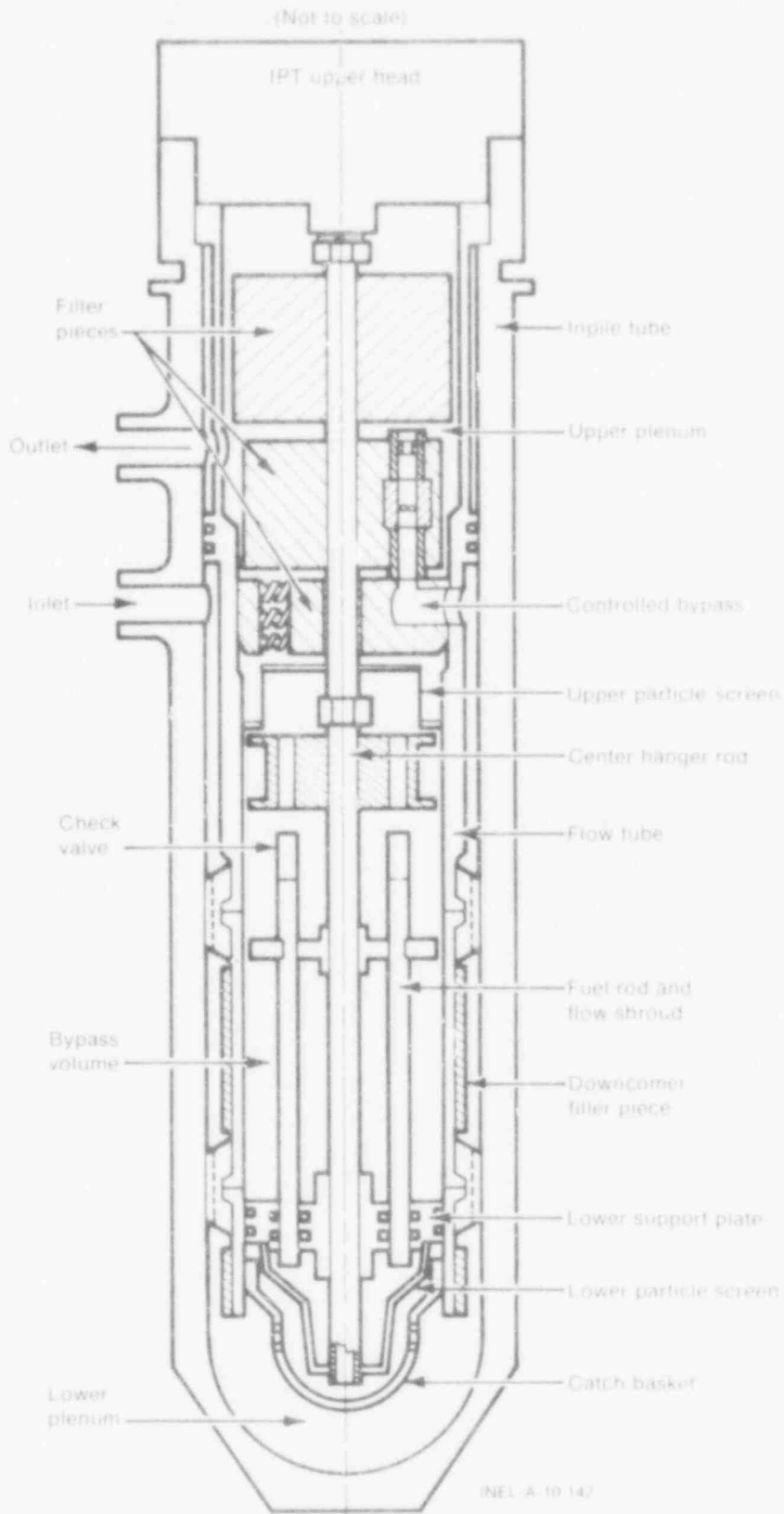
Fig. 2 PBF LLR test train illustration.

15.65 MPa pressure and 562.5 K inlet temperature conditions. The hole is approximately 31.8 mm in diameter and is drilled in the IPT flow tube at the elevation of the IPT inlet, but 180 degrees around the flow tube from the inlet. The bypass includes the capability of being orificed to reduce flow area and is metered with a flow turbine.

2.4 PBF-LOCA Blowdown System

The PBF-LOCA blowdown loop is illustrated in Figure 3. The blowdown system provides a flow path during steady state pre-blowdown operation and provides the means to isolate the IPT from the existing loop during blowdown so the loop can continue to operate through the bypass line. Blowdown through the Henry nozzles can be effected through either the cold leg or the hot leg or both, and is initiated and controlled by means of quick opening and closing blowdown valves. The nominal response time required for the blowdown valves is 70 ms from closed to fully open. The four Henry nozzles provide the break plane, break flow rate, and depressurization rate. The final throat areas and locations utilized for these nozzles for the PBF/LLR Tests are tabulated in Table III. By selective sequencing of the blowdown valves, the LOFT required depressurization was obtained for the tests.

TABLE III

PBF/LOFT LEAD ROD TEST BLOWDOWN LOOP HENRY NOZZLE THROAT DIAMETERS AND LOCATIONS

Nozzle Designation	Location	Throat Diameter, mm	Utilized for Test
FE-11-1-2	Hot Leg	13.56	LLR-3
FR-LR-C-1 (replaced FE-11-1-3)	Cold Leg	12.47	LLR-3,4.5,4A
FE-LR-C-2 (replaced FE-11-1-4	Cold Leg	23.90	LLR-3,4,5,4A

480 146

9
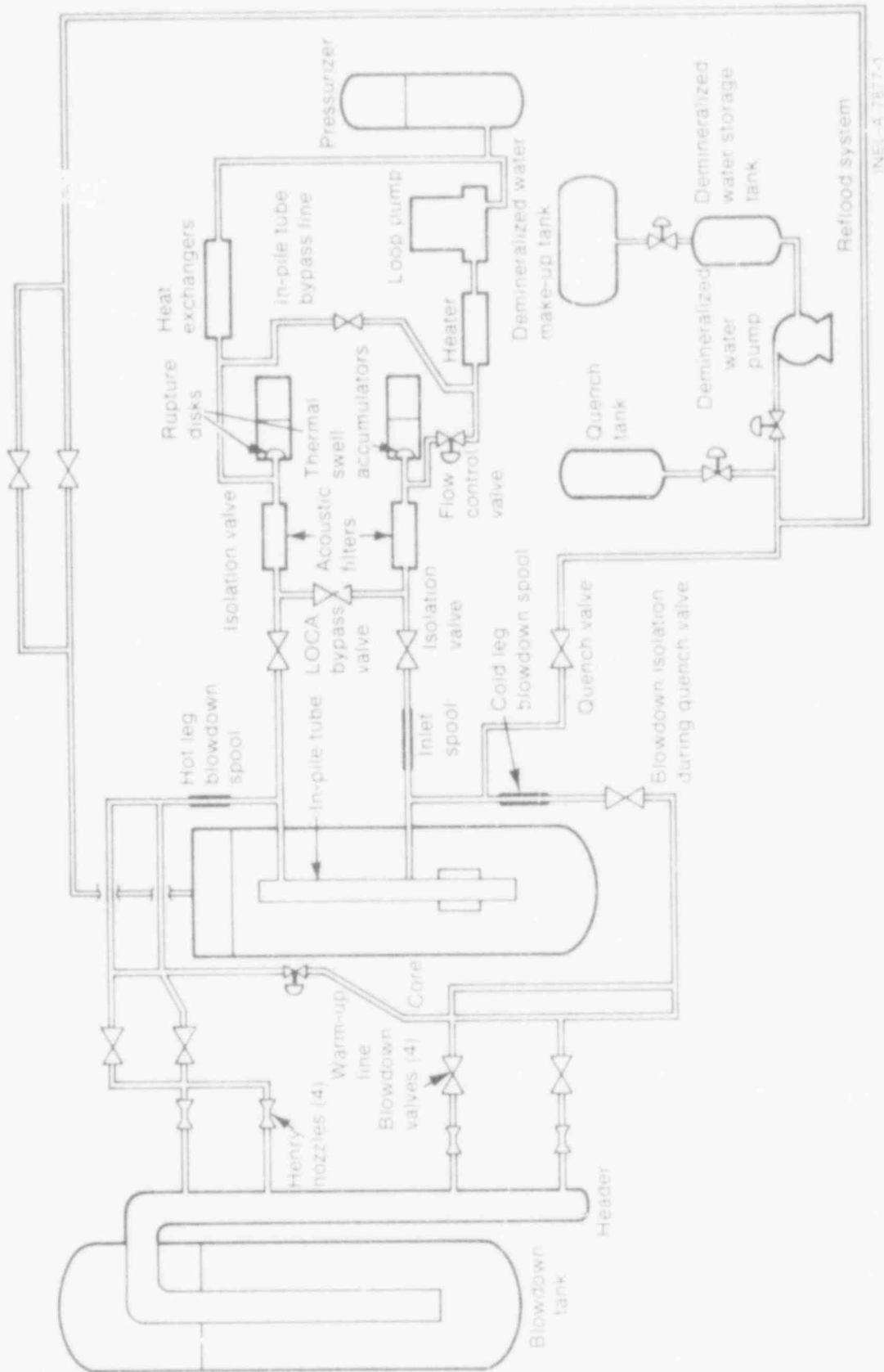
Fig. 3 PBF/LOCA blowdown loop.

A small line connects the hot and cold blowdown piping legs with a controllable valve (warmup line and valve). This line provides a small flow rate to keep the legs at a constant temperature prior to blowdown.

The blowdown header and tank collect and contain the coolant ejected from the IPT and piping during blowdown, reflood, and quench, as well as any fission products carried from the fuel rods by the coolant, in the event of rod failure.

With the completion of the reflood portion of the transient, posttest quench cooling is accomplished by opening the quench valve (and closing the cold leg blowdown valves) to permit coolant from the quench tank to enter the IPT. The quench tank is pressurized to 1.37 MPa by a nitrogen gas system and heated to approximately 366 K.

The LOCA system contains an initial condition measurement spool and a blowdown measurement spool in each blowdown leg. The instrumentation for the system is described in Section 2.5.

Sequencing of the valve operation during blowdown is controlled by a time-sequential programmer in the Programming and Monitoring System (P&MS).

Further information on the PBF/LOCA blowdown system is available in Reference 7.

2.5 Experiment Instrumentation

The experiment instrumentation for the PBF/LLR tests consists of devices to measure the fuel rod surface and centerline temperatures, plenum pressure and temperature, and axial length change (LVDT). Devices to measure the coolant pressure, temperature, density, and flow rate are also included. The instrumentation utilized for the fuel trains, test train, and inlet conditions and blowdown measurement spools is described in Tables IV, V, and VI.

480 148

TABLE IV

INSTRUMENTATION UTILIZED FOR THE LLR FUEL TRAINS FOR TEST LLR-4A

Measurement	Designation	Rod Number	Comments
			LOFT laser welded technique:
	CLAD3992bb-1400008	8	0.314 m elevation 0° azimuthal
Cladding	CLAD3992bb-0018008	8	0.457 m elevation 180° azimuthal
Surface	CLAD3122bb+0818002	2	0.533 m elevation 180° azimuthal
Temperature	CLAD3122bb+0000002	2	0.457 m elevation 0° azimuthal
(thermocouple)	CLAD3451bb+0818005	5	0.533 m elevation 180° azimuthal
	CLAD3451bb+0800005	5	0.533 m elevation 0° azimuthal
Fuel	TFCL3992bb+.00TC08	8	0.457 m elevation
Centerline	TFCL3122bb+.00TC02	2	0.457 m elevation tungsten-rhenium
Temperature	TFCL3451bb+.08TC05	5	0.533 m elevation
(thermocouple)	TFCL3452bb+.00TC06	6	0.457 m elevation
Cladding	LVDTbRODbb312-1b01	1,8	
Elongation	LVDTbRODbb312-2b02	2	Linear variable differential
(LVDT)	LVDTbRODbb312-3b03	3,5	transformers of EG&G Idaho,
	LVDTbRODbb312-4b04	4,6	Inc. design and manufacature.
Plenum	RODPRESSbb399-2R08	8	
Pressure	RODPRESSbb312-2R02	2	Kaman eddy current type
(transducer)	RODPRESSbb345-1R05	5	
	RODPRESSbb345-2R06	6	
Plenum	PLNMTEMPhb399-2R08	8	
Temperature	PLNMTEMPbb312-2R02	2	
(thermocouple)	PLNMTEMPbb345-1R05	5	
	PLNMTEMPbb345-2R06	6	
Coolant	INLTTEMPbb399-2R08	8	
Bulk	INLTTEMPbb312-2R02	2	Inlet of each flow shroud
Temperature	INLTTEMPbb345-1R05	5	Grounded thermocouples
(thermocouple)	INLTTEMPbb345-2R06	6	
	OUTbTEMPbb399-2R08	8	
	OUTbTEMPbb312-2R02	2	Outlet of each flow shroud
	OUTbTEMPbb345-1R05	5	
	OUTbTEMPbb345-2R06	6	
	MIDT3992bb+.000R08	8	
	MIDT3992bb-.120R08	8	
	MIDT3992bb+.120R08	8	
	MIDT3451bb+.000R05	5	
	MIDT3451bb-.120R05	5	
	MIDT3451bb+.120R05	5	

TABLE IV (continued)

Measurement	Designation	Rod Number	Comments
Coolant Differential Temperature (thermocouple)	DELT3122bb225bbR02 DELT3992bb225bbR08 DELT3451bb225bbR05 DELT3452bb225bbR06 R2DTCVSPR02	2 8 5 6 2	Yield temperature increase across each flow shroud for power calibration purposes Ungrounded thermocouples
Flow Shroud Temperature (thermocouple)	TSRD3451bb+.000R05 TSRD3451bb-.120R05 TSRD3451bb+.120R05 TSRD3992bb+.000R08 TSRD3992bb-.120R08 TSRD3992bb+.120R08	5 5 5 8 8 8	At midplane and 120 mm above and below the midplane Grounded thermocouples
Coolant Volumetric Flow Rate (turbine meters)	TURB3121bbUP000N01 TURB3122bbUP180N02 TURB3123bbUP090N03 TURB3124bbUP270N04	8 2 5 6	Flow Technology bi-directional flow meters at inlet of each flow shroud
	TURB3121bbL0000N01 TURB3122bbL0180N02 TURB3123bbL0090N03 Turb3124bbL0270N04	8 2 5 6	Outlet of each flow shroud
Fuel Rod Power Profile (flux wires)	FLUXHRODbb-46315TT FLUX3122bb-4609002 FLUX3451bb-4609005 FLUX3452bb-4609006 FLUX3992bb-4609008	TT 2 5 6 8	Aluminum-colbalt alloy flux wires located on the outside of each shroud and one on the hanger rod. These devices will give the time integrated axial power distribution in the rod.

(b denotes blank)

Measurements	Designation	Comments
Coolant Bulk Temperature (thermocouple)	BULKTEMPbbCATCHBTT	Coolant temperature in catch basket in lower plenum.
	BULKTEMPbbLOWSPTTT	Coolant temperature at lower support plate in lower plenum.
	BULKTEMPbbVOLBYPTT	Coolant temperature in volumetric bypass in lower plenum.
	BULKTEMPbbSRDOUTTT	Coolant temperature at the outlet of the four flow shrouds.
	BULKTEMPbbIPTEXTTT	Coolant temperature at the IPT outlet nozzle.
	BULKTEMPbbCONTBYTT	Coolant temperature in the controlled bypass.
Coolant Pressure (transducer)	PRESSUREbbECATCHTT	EG&G Idaho, Inc. strain post transducer in catch basket in lower plenum.
	PRESSUREbbETOPSPTT	EG&G Idaho, Inc. strain post transducer at top support plate in upper plenum.
	PRESSUREbbKTOPSPTT	Kaman eddy current transducer at top support plate in upper plenum.
	PRESS-HIbbECATCHTT	EG&G Idaho, Inc. strain post transucer for overpressure in catch basket in lower plenumn.
Neutron Flux (self powered Neutron Detectors)	NEUTFLUXbb+.342bTT	Reuter-Stokes cobalt detectors. Spaced along the length of the active core region at 135° from north. Will be utilized to correlate reactor power to calibrated fuel rod power and determine the axial power shape with power level.
	NEUTFLUXbb+.228bTT	
	NEUTFLUXbb+.142bTT	
	NEUTFLUXbb+.000bTT	
	NEUTFLUXbb-.114bTT	
	NEUTFLUXbb-.228bTT	
	NEUTFLUXbb-.342bTT	
Relative Gamma Flux (gamma detectors)	GAMMAFLXbb+228bbTT	Reuter-Stokes platinum detectors at core centerline and 228 mm above and below the midplane.
	GAMMAFLXbb+000bbTT	
	GAMMAFLXbb-228bbTT	
Liquid Level Detectors	LIQLEVELbb312-1R01	Two below the lower support plate and one in each flow shroud below the rod. EG&G Idaho, Inc. heated design.
	LIQLEVELbb312-2R02	
	LIQLEVELbb312-3R03	
	LIQLEVELbb312-4R04	
	LIQLEVELbbLOSUPTT1	
	LIQLEVELbbLOSUPTT2	
Controlled Bypass Volumetric Flow Rate (turbine-meter)	TURBINEMbbCONTBYTT	In controlled bypass piping. Flow Technology turbine meter.

14

480-451

TABLE VI

INSTRUMENTATION UTILIZED FOR THE PBF/LLR HOT LEG, COLD LEG, AND INITIAL CONDITIONS SPOOL PIECES

Measurements	Designation	Comments
Coolant Volumetric Flow Rate (Turbine meters)	ICSVFLOWbbFE05SPIC CLSVFLOWbbFE06SPCL HLSVFLOWbbFE09SPHL	Full flow turbine meters from Flow Technology, Inc.
Coolant Momentum Flux (Drag disk)	CLMOMFLXbbFE07SPCL HLMOMFLXbbFE08SPHL	Rampo, Inc., transducer.
Steady-State Coolant Bulk Temperature (RTD)	ICSSTEMPbbTE20SPIC CLSSTEMPbbTE22SPCL HLSSTEMPbbTE23SPHL	Rosemount resistance temperature detectors.
Transient Coolant Bulk Temperature (ribbon T/C)	ICTCTEMPbbTE21SPIC CLTCTEMPbbTE24SPCL HLTCTEMPbbTE25SPHL	Rosemount Type K ribbon thermocouples.
Subcooled Coolant Pressure Flush Mounted (transducer)	ICPRESSFbbPE08SPIC CLPRESSFbbPE10SPCL HLPRESSFbbPE12SPHL	Precise Sensors transducers.
Saturated Coolant Pressure (water cooled transducer)	ICPRESSWbbPE09SPIC CLPRESSWbbPE11SPCL HLPRESSWbbPE13SPHL	Precise Sensors transducers.
Coolant Pressure Differential (hot leg to cold leg spool (transducer)	DELPCLHLbbDPE-05HL	This device from BLH measures the pressure difference across the test train.
Coolant Density (Gamma Densitometer)	CLDENSUPbbDENS1UCL CLDENSCEbbDENS1CCL CLDENSLObbDENS1LCL HLDENSUPbbDENS2UHL HLDENSCEbbDENS2CHL HLDENSLObbDENS2LHL	EG&G Idaho, Inc. design and manufacutre.

480 152

3. EXPERIMENT DESCRIPTION AND CONDUCT

3.1 Description of PBF/LLR Test Program

A summary of the PBF/LLR test program and fuel behavior results
is presented in this section. The program was designed to simulate
the LOFT L2 Power Ascension Test Series for Tests L2-3 through L2-5
during the pretest steady state preconditioning operation, the LOCE
transient, and reflood. Test LLR-4A was a follow-on test to the
original program. The LLR tests sequentially tested selected fuel
rods to determine the effect of successive LOCE transients on the LOFT
center (high power) and peripheral (low power) assembly fuel rods.
The structuring of the program provides a parametric evaluation of
LOFT fuel rod behavior over a wide range of power densities
(34.2-52.5 kW/m, 12.0-16.0 kW/ft).

Test LLR-3 initiated the PBF/LLR program at the rod powers
designated for the LOFT L2-3 test. For Test LLR-3, Rods 312-1 and
312-2 were surrounded by zircaloy shrouds to be representative of the
LOFT high power rods, and Rods 312-3 and 312-4 were surrounded by
stainless steel shrouds to be representative of the LOFT low power
(peripheral) rods. The desired linear peak powers for the high power
and low power fuel rods were approximately 39.27 kW/m (12 kW/ft) and
34.55 kW/m (10.43 kW/ft) repectively. The measured high power test
rod peak powers were calculated to be slightly higher (40 kW/m peak)
than these desired peak powers. Rod 312-3, which was a low power rod,
failed during the test due to attaining a waterlogged condition prior
to the blowdown. Measured cladding temperatures attained during the
transient were: rod 312-1, 950 K; rod 312-2, 925 K; rod 312-3,
1005 K; and rod 312-4, 870 K. No mechanical deformation occurred to
the fuel rods at these temperature levels.

Following the LLR-3 Test, the two low power fuel rods were
replaced with fresh (zircaloy shrouded) fuel rods designated
Rods 345-1 and 345-2. In keeping with the planned test sequence for
LOFT, Test LLR-5 then preceded Test LLR-4, and involved a second test

cycle at approximately 46 kW/m for rods 312-1 and 312-2 previously used in Test LLR-3, and the first cycle for the fresh rods (345-1 and 345-2) at approximately the same high power condition. Test LLR-5 utilized a delayed PBF driver core scram of 2.0 seconds into the blowdown in an attempt to reach higher cladding surface temperatures. Measured cladding temperatures attained during the transient were: rod 312-1, 995 K; rod 312-2, 1015 K; and rod 345-1, 1005 K. Rod 345-2 was not instrumented with cladding thermocouples. No mechanical deformation occurred to the fuel rods at these temperature levels.

Test LLR-4 then involved a third test cycle for the zircaloy shrouded Rods 312-1 and 312-2, and a second test cycle for the fresh zircaloy shrouded rods of test LLR-5 (Rods 345-1 and 345-2) at a desired maximum linear peak power of 52.5 kW/m (16 kW/ft). The actual test rod powers were calculated to be slightly higher (56 kW/m) than this desired peak power. This test corresponds to the high power condition for the LOFT tests. Utilizing a 2.6 second delayed scram on the driver core to attain higher cladding temperatures, measured cladding temperatures attained for the rods were: rod 312-1, 1130 K; rod 312-2, 1170 K; and rod 345-1, 1060 K. At these cladding temperatures, rods 312-1 and 312-2 are expected to have reached the waisting regime of mechanical deformation while rod 345-1 is expected to have reached the buckling regime.

The primary purpose of the PBF/LLR tests was to achieve the maximum mechanical deformation that could possibly occur to the LOFT fuel during the Power Ascension tests, and then investigate the effect of power ramping and additional blowdowns on the deformed rods. Since fuel rod mechanical deformation was not achieved until the LLR-4 test, the LLR-4A test was conducted to meet this objective. Test LLR-4A was conducted at the same test conditions as Test LLR-4. It involved the fourth test cycle for rod 312-2, the third test cycle for rods 345-1 and 345-2, and the first test cycle for rod 399-2 at a desired maximum linear peak power of 52.5 kW/m (16 kW/ft). The actual test rod powers were calculated to be slightly higher (56 kW/m) than this desired peak power. Utilizing a 2.85 second delayed scram on the driver core,

measured cladding temperatures attained for the rods were: rod 399-2, 1260 K; rod 312-2, 1150 K; and rod 345-1, 1075 K. At these cladding temperatures, rods 399-2 and 312-2 are expected to have reached the waisting regime of mechanical deformation while rod 345-1 is expected to have reached the collapse regime. It should be noted that the peak temperature on Rod 399-2 was measured at the .314 m location. The remaining temperatures in this test and in the previous LOFT lead rod tests were measured at (or slightly above) the peak power location (0.457 m).

3.2 Experiment Conduct

The LLR-4A test consisted of six phases: (1) heat up; (2) power calibration; (3) decay heat buildup; (4) blowdown; (5) reflood; (6) quench and cooldown.

Experiment operation began with the nonnuclear heatup of the IPT loop coolant system by coolant circulation with the loop pump. Following the heatup phase, nuclear operation commenced. Power calibrations at several intermediate power levels were performed and nuclear operation was continued until the initial conditions identified in Table VII for the test were attained. At this point, the blowdown portion of the transient was initiated, followed by the reflood and quench phases of the test.

The following sections describe the test conduct during each phase in more detail.

3.2.1 Heatup Phase. During the heatup phase, system conditions and experimental measurements were monitored to evaluate instrument performance.

3.2.2 Power Calibration Phase. The power calibration phase of the test consisted of several slow power ramps from low powers to successively higher powers. During the slow power ramps, and at specific steady state power levels, test rod powers were determined by

480 155

TABLE VII

INITIAL CONDITIONS FOR THE PBF/LLR-4A TEST PRIOR TO BLOWDOWN

Test	Reactor Power[a] (MW)	MLHGR[b] (kW/m)	System Pressure[c] (MPa)	IPT Inlet Temperature[d]	Average Core Differential Temperature[e]	Shroud Flow[f] (1/s)
LLR-4A	19.3	55.6	15.5	600.0	11.5	0.78

(a) Reactor Power based on NMS-3 ion chamber (console reading)
(b) Maximum Linear Heat Generation Rate (zircaloy shrouded rods calculated average)
(c) Recorded at the Heise gauge in the primary coolant system
(d) Recorded with the initial conditions spool piece RTD
(e) Zircaloy shrouded rods average
(f) Flow per flow shroud

thermal-hydraulic calculations based on flow, differential temperature, inlet temperature, and pressure. These test rod powers were then intercalibrated with reactor power (NMS-3) to determine the figure-of-merit (FOM) for the test rods in the PBF IPT.

A ramp rate similar to that LOFT will use during the L2 Tests was utilized for the LLR-4A test. Figure 4 shows the reactor operational sequence followed during the test. Power calibrations were conducted at steady state driver core power levels of 4.8, 9.8, 14.5, and 19.3 MW for Test LLR-4A. Results from these power calibrations are given in Table VIII. An axial peaking factor of 1.34 was utilized in the calculations of rod peak powers.

The peak test rod calculated figure of merits (FOM) (peak rod power divided by PBF core power) are also listed in Table VIII. These values are useful from a reactor operation viewpoint, but are mediocre indicators of test rod power because of nonlinearaties and IPT coolant temperature effects. Therefore, the power calibration is designed to provide only an approximate envelope for reactor power.

3.2.3 Decay Heat Buildup Phase. After completion of the power calibration phase, the test fuel rod peak power was maintained at a steady state level of 55.6 kW/m for an additional 3 hours. This length of time was necessary to build up approximately 82% of the maximum possible decay heat in the rods.

3.2.4 Blowdown, Reflood, and Quench and Cooldown Phase for Test LLR-4A. At 3:05 p.m May 18, 1979, the blowdown was initiated for Test LLR-4A. At time zero the blowdown was initiated by opening both cold leg blowdown valves. A delayed scram of 2.85 seconds was utilized for this test to attain cladding temperatures comparable to those attained in Test LLR-4. Driver core power during this time period was controlled with the transient rod servo-controller. The system valves
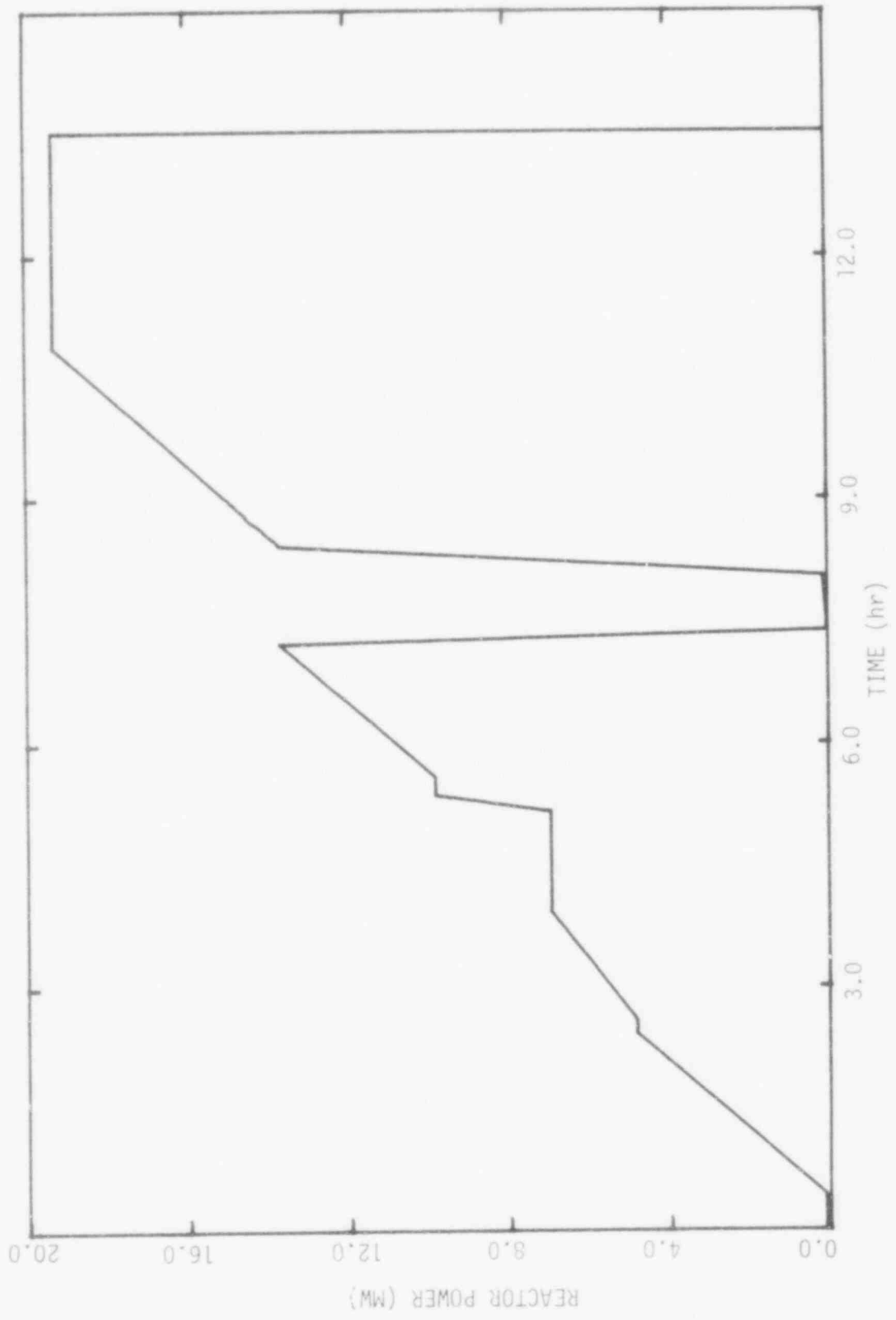
Fig. 4 Reactor power history test LLR-4A.

TABLE VIII

SUMMARY OF POWER CALIBRATION FOR TEST LLR-4A

Rod[a]	NMS-3 Reactor Power (MW)	Inlet Temp[b,c] K	Coolant Δ T K	Coolant Flow 1/s	Test Rod Power Peak (kW/m)	Average (kW/m)	FOM[d] (kW/m/MW)
8	4.8	587.4	3.53	0.775	16.67	12.52	3.44
2	4.8	587.4	3.51	0.800	17.21	12.84	3.56
5	4.8	587.4	3.45	0.815	17.22	12.85	3.56
8	9.8	587.0	6.69	0.769	31.84	23.76	3.25
2	9.8	587.0	6.40	0.797	31.54	23.54	3.22
5	9.8	587.0	6.40	0.809	31.98	23.87	3.25
8	14.5	587.4	9.06	0.774	43.88	32.74	3.02
2	14.5	587.4	8.57	0.803	42.97	32.07	2.96
5	14.5	587.4	8.68	0.815	43.70	32.61	3.01
8	19.3	601.3	9.98	0.758	53.15	39.67	2.75
2	19.3	601.3	9.24	0.783	50.55	37.72	2.62
5	19.3	601.3	9.57	0.795	53.26	39.75	2.76

(a) Rod 8 = Rod 399-2, Rod 2 = Rod 312-2, Rod 5 = Rod 345-1.   Rod 6 (Rod 345-2) did not have an operable differential thermocouple during the test.

(b) Inlet conditions spool piece RTD.

(c) Coolant inlet pressure (Heise Gauge,   5.6 MPa.

(d) Based on NMS-3 digital power readout on display console.

sequenced as shown in Table IX through the reflood portion of the transient. Quench injection for long term cooling was initiated at 239 seconds into the transient, and was followed by continued flow from the hot water and storage tanks.

TABLE IX

PROGRAMMING AND MONITORING SYSTEM CONTROLLED EVENT SEQUENCE FOR TEST LLR-4A

Step	REDCOR Signal Initiated Time (s)	Event Initiated Time (a) (s)	Loop Bypass Valve(c)	Two PCS Isolation Valves(d)	Hot Leg Blowdown Valve 1(e)	Hot Leg Blowdown Valve 2(f)	Cold Leg Blowdown Valve C1(g)	Cold Leg Blowdown Valve C2(h)	Quench Water Valve(i)	Warm-Up Line Valve(j)	Cold Leg Shutoff Valve(k)
Initial	--	--	X(b)	0	X	X	X	X	X	0	0
Initial	(1)	(1)	X	0	X	X	X	X	X	X	0
1	-0.070	0.00	0	X	X	X	X	X	X	X	0
2	0.03	0.10	0	X	X	X	0	0	X	X	0
3	3.68	3.75	0	X	X	X	0	X	X	X	0
4	22.03	22.10	0	X	X	X	0	0	X	X	0
5	reflood cycle	120.0	0	X	X	X	0	0	X	X	0
6	quench and cooldown	239.0	0	X	0	0	X	0	0	X	X

(a) A 70-ms delay is expected in the valve solenoids
(b) X indicates closed, 0 indicates open
(c) Valve VALVbPOSbbLM1107PT
(d) Valves VALVbPOSbbLM1105PT and VALVbPOSbbLM1106PT
(e) Valve VALVbPOSbbLM1101PT
(f) Valve VALVbPOSbbLM1102PT
(g) Valve VALVbPOSbbLMRC1PT (Henry Nozzle FR-LR-C-1)
(h) Valve VALVbPOSbbLMRC2PT (Henry Nozzle FR-LR-C-2)
(i) Valve VALVbPOSbbLM1108PT
(j) Valve VALVbPOSbbLM1116PT
(k) Valve VALVbPOSbbLM1118PT. This valve is not actuated by the P&MS System.
(1) Prior to blowdown the warm-up line valve was closed and flow was reestablished to the steady-state flows designated in Table VII for the flow shrouds, before the blowdown switch was activated.

24

4. PRELIMINARY RESULTS AND COMPARISON WITH PREDICTIONS FOR PBF/LLR TEST LLR-4A

The following sections describe the loop coolant and fuel rod behavior for the PBF/LLR Test LLR-4A and provide preliminary comparisons of these measured results with calculations made with the RELAP4/MOD6[8](a) and the FRAP-T5[9](b) codes. The RELAP4 pretest predictions were performed using a special version of the code which is described in Reference 10. RELAP4 was used to calculate the loop thermal-hydraulic behavior and to generate a coolant mass flux, pressure, and enthalpy boundary condition for the FRAP code. Both RELAP4 and FRAP consistently predicted shorter times to CHF than the measured data, as exemplified in Figure 18 for rod 312-1, and this resulted in maximum predicted cladding temperatures 200 to 350 K higher than the measured data for all cases. Therefore, complete comparisons of predicted cladding temperature versus measured cladding temperature are not presented in this report.

It should be noted that the experimental data presented in this report are preliminary and have not been qualified. In some cases offsets have been applied to the data.

4.1 Loop Coolant Behavior for Test LLR-4A

Test LLR-4A was conducted at the initial system conditions described in Table VII, with a peak linear heat generation rate just prior to blowdown of 56 kW/m, and with the valve sequencing described in Table IX. The pretest RELAP4 predictions were made assuming a fuel rod peak linear heat generation rate of 52.5 kW/m for the four zircaloy shrouded rods, an IPT inlet temperature of 595 K, an IPT

(a) RELAP4/MOD6. Idaho National Engineering Laboratory Configuration Control Number H004461IB.

(b) FRAP-T5. Idaho National Engineering Laboratory Configuration Control Number H007441IB.

inlet pressure of 15.5 MPa, and fuel rod shroud flows of 0.78 1/s per shroud. For all practical purposes the initial conditions and sequencing of the test relative to the RELAP4 pretest predictions were the same.

Figure 5 shows the RELAP4 calculated system depressurization compared with experimental data from the initial conditions spool piece pressure transducer. With a 0.5 MPa offset applied, the data indicate a subcooled depressurization to approximately 11.75 MPa. This corresponds to a saturation temperature of 596 K. The inlet conditions RTD was maintained at 600 K prior to blowdown in an effort to keep the dead legs to the hot and cold leg blowdown valves at 595 K. As shown, measured system depressurization during the blowdown matched the predicted response extremely well.

Figure 6 compares the predicted and measured coolant temperatures at the cold leg spool piece. As shown, the measured coolant temperature follows the depressurization saturation line trends set forth by RELAP4 for the entire transient.

Figure 7 presents the predicted pressure differential between the hot and cold leg blowdown spools. Measured pressure differences between the hot and cold leg blowdown spool are not available because the instrument failed just prior to the blowdown. However the actual values should be similar to data presented in Reference 11 for Tests LLR-3 and LLR-5. At steady state, the cold leg spool piece pressure was approximately 0.2 MPa higher than the hot leg spool piece pressure. When blowdown was initiated, the pressure differential reversed, resulting in a 0.55 MPa differential from the upper plenum to the lower plenum. This pressure differential rapidly closed the check valves on the top of each flow shroud, resulting in rapid coolant voiding and a saturated steam environment for each fuel rod. At approximately 4 seconds into the transient, the pressure difference decreased sharply to 0.04 MPa and remained constant for the remainder of the blowdown transient.
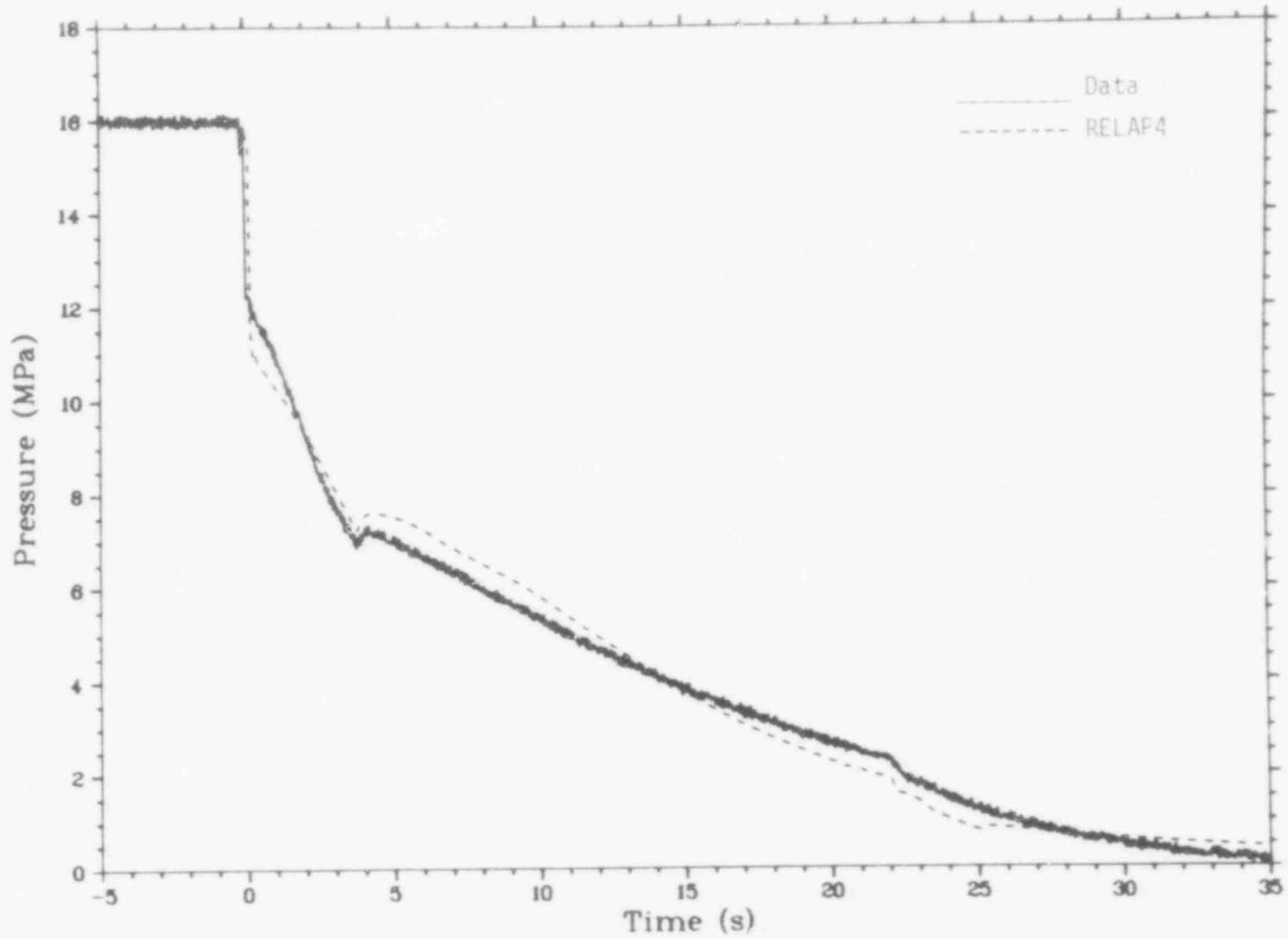
Fig. 5 Test LLR-4A comparisons between analytical and experimental system depressurization in the initial conditions spool piece.
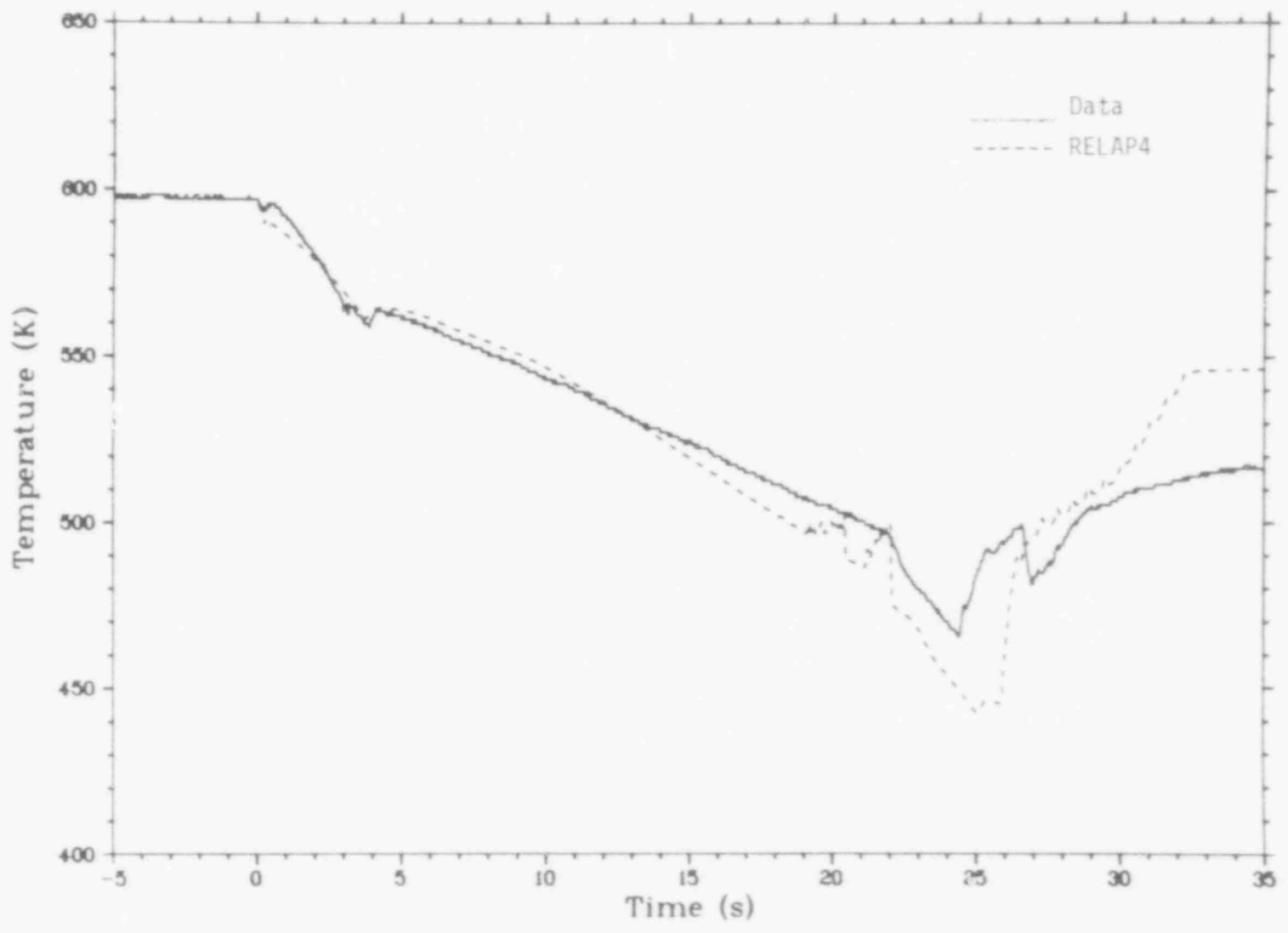
27

Fig. 6 Test LLR-4A comparisons between analytical and experimental cold leg spool
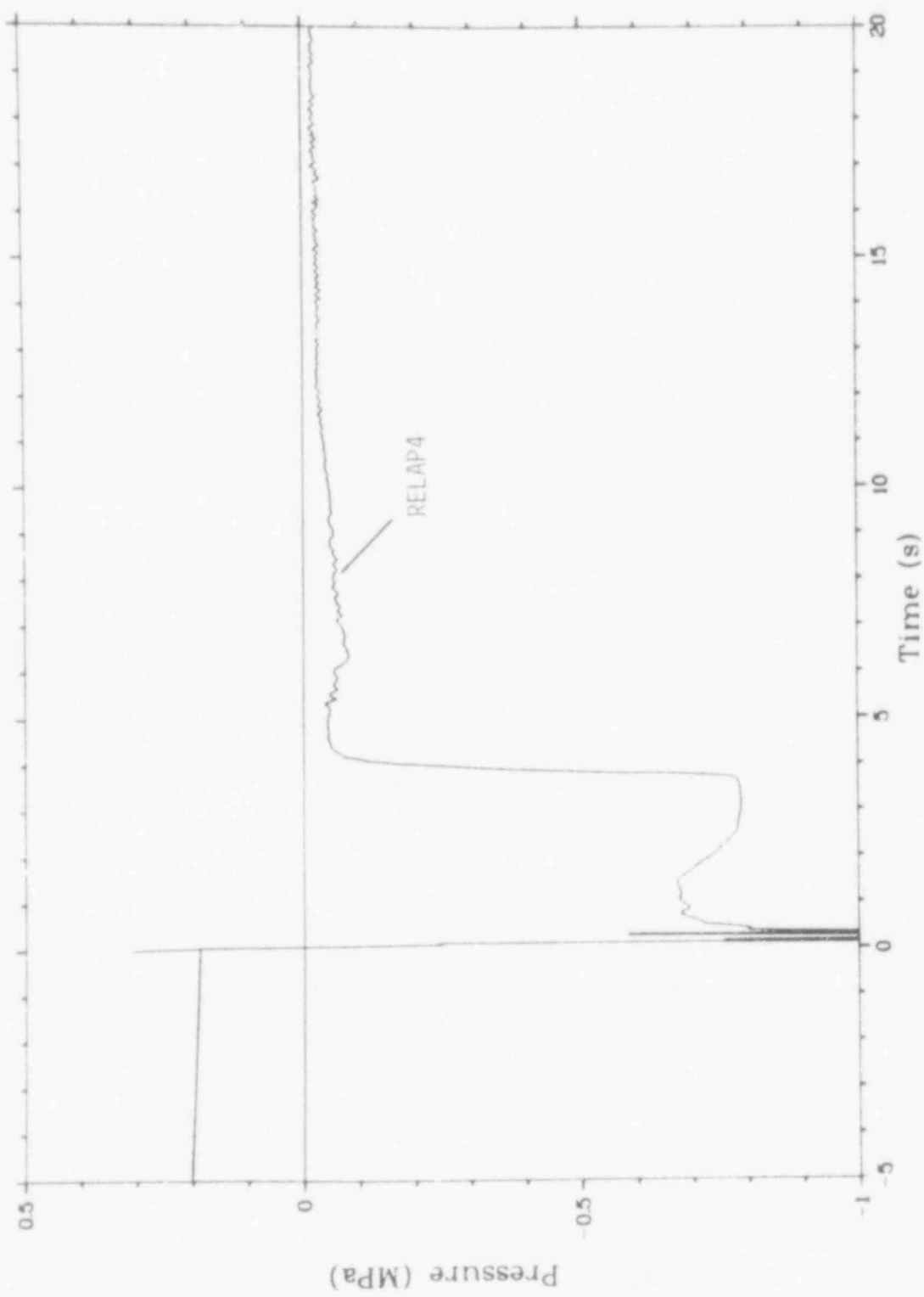piece temperatures.

28

Fig. 7 Test LLR-4A analytical cold leg to hot leg differential pressure.

Figure 8 shows a comparison of the predicted and measured volumetric flow rate at the cold leg blowdown spool piece. Upon completion of the test, it was discovered that the turbine blades were severly damaged on this flowmeter. The measured flow rates are less than the RELAP4 predictions for the entire blowdown transient. In the three prior tests, the measured volumetric flow rate followed the predicted flow rate extremely well. The predicted flow, therefore, presents a closer representation of the thermal-hydraulics that occured in the IPT. At initiation of blowdown, the measured initial flow spike indicates 60 l/s. With the completion of the subcooled portion of the blowdown, the Henry nozzles cause choked flow to result almost instantaneously. With choked flow established, the measured volumetric flow decreased to approximately 40 l/s within about 1.0 second. The volumetric flow then increased to 59.5 l/s at about 4 seconds after blowdown. The increase in flow was due to the continually decreasing coolant density as the system depressurized, resulting in high void fraction steam mixtures.

Figure 9 shows the predicted and measured coolant density as a function of time at the cold leg spool piece. The experimental curve is based on data obtained from all three beams of the three-beam gamma densitometer. The RELAP4 prediction compares well with the experimental data. Beyond approximately 5.0 seconds, the data exhibits a slightly higher measured density.

Figure 10 compares the predicted and measured mass flow rate at the cold leg spool piece. The measured mass flow rate was derived from a gamma densitometer/turbine meter (cold leg) combination. As shown, with the damaged turbine meter indicating a lower volumetric flow than expected, the RELAP4 predictions overpredicts the measured mass flow rate from initiation of blowdown until 5 seconds. Beyond this point the predicted mass flow rate is slightly higher than the measured value. Comparison of this parameter for prior tests indicated excellent comparison between measured and predicted mass flow.
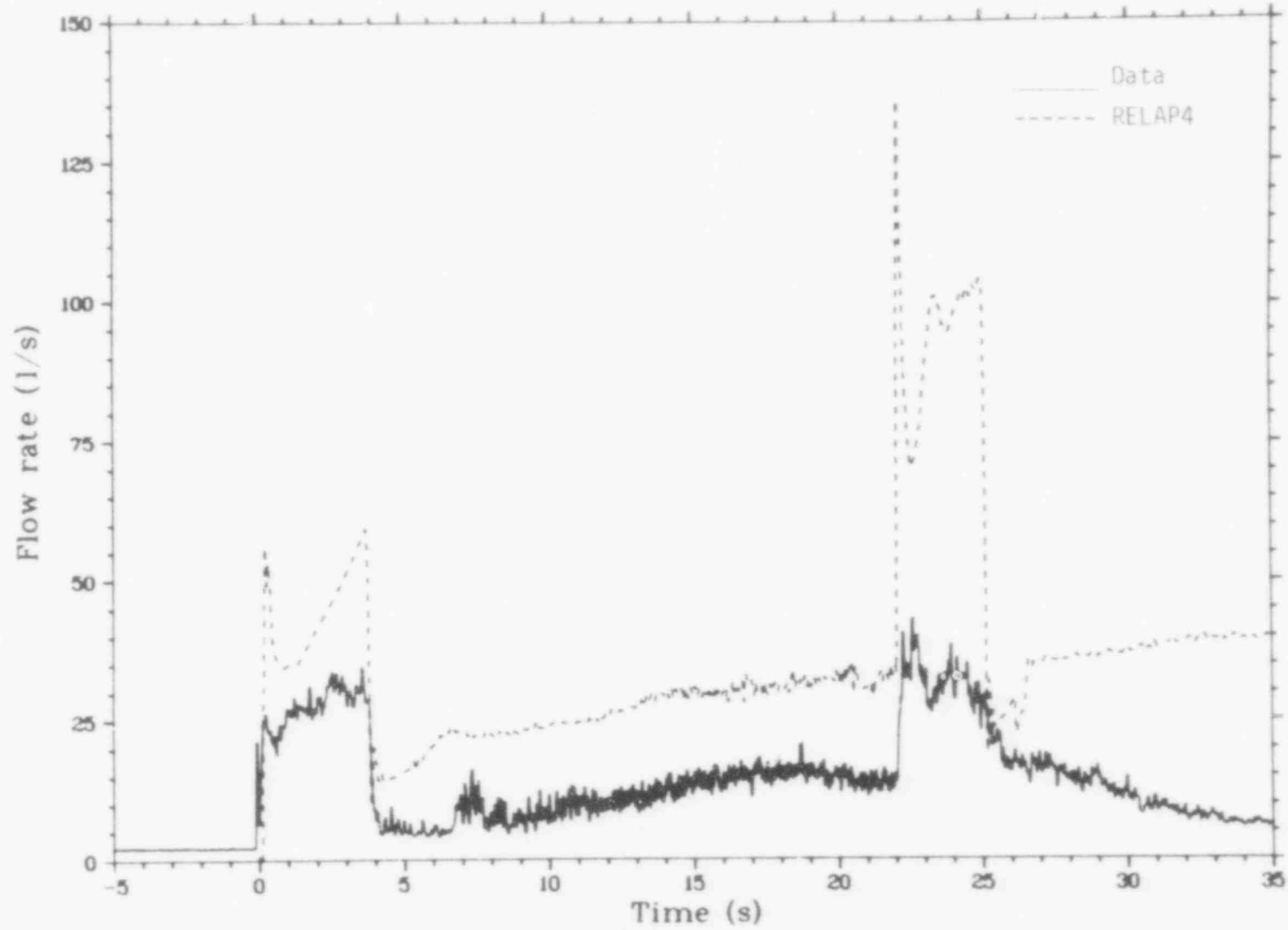
30

Fig. 8 Test LLR-4A comparisons between analytical and experimental volumetric flow
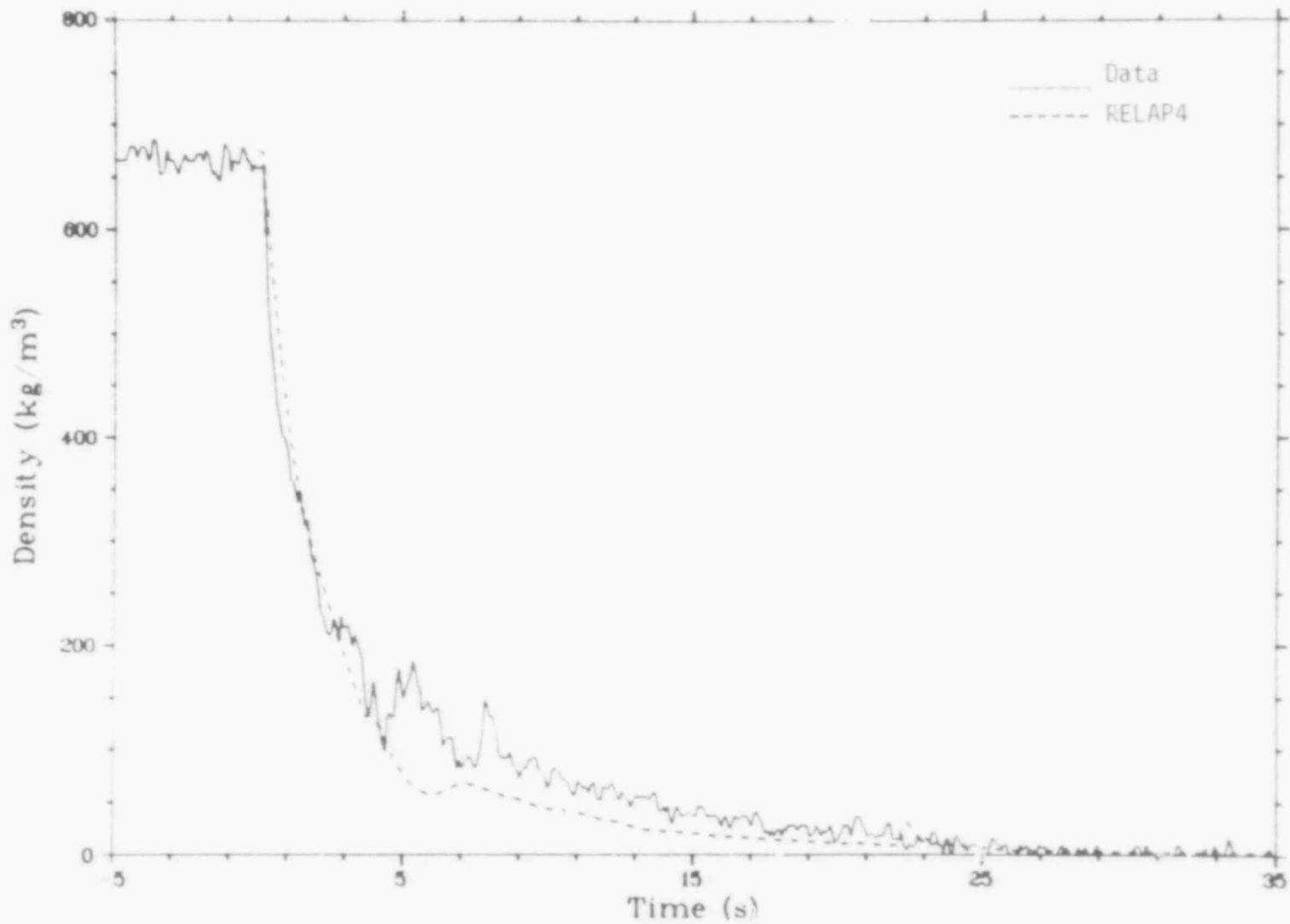rates in the cold leg spool piece.

Fig. 9 Test LLR-4A comparisons between analytical and experimental cold leg
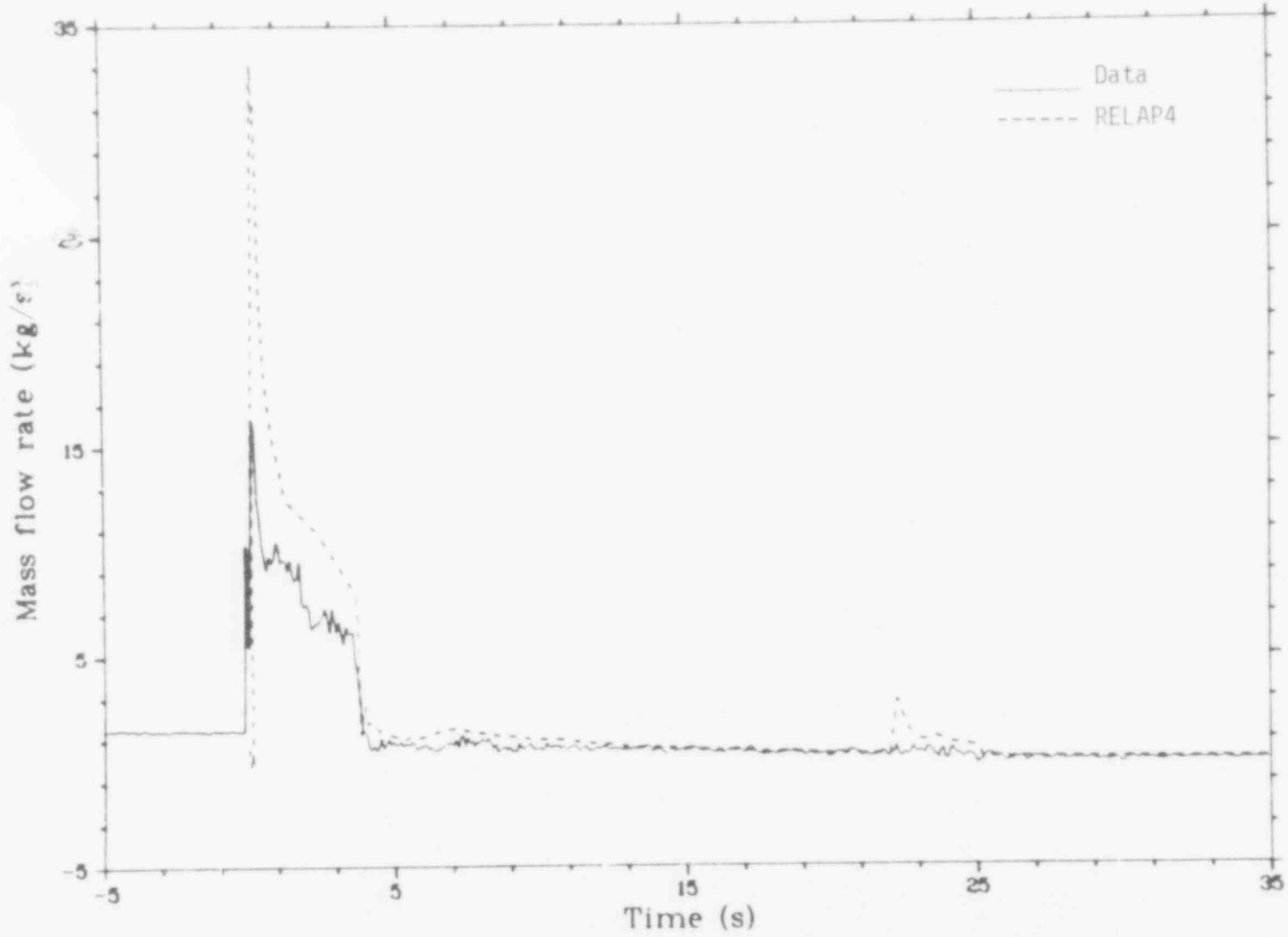spool piece densities.

Fig. 10 Test LLR-4A comparisons between analytical and experimental cold leg spool piece mass flows.

The controlled bypass turbine meter failed prior to the LLR-4A blowdown. It is assumed that the flow response of this instrument follows the trends seen in Test LLR-4. As shown in Figure 7, the change in differential pressure forces the shroud check valves closed for the entire transient. This valve closure forces the two-phase mixture in the upper plenum out the controlled bypass flow path to the cold leg. As shown in Figure 11, RELAP4 significantly underpredicted the amount of flow leaving the upper plenum for Test LLR-4. Thus, since the differential pressure across the spool pieces was matched relatively well and the measured volumetric flows were much higher than predicted, the code did not predict the correct phase separation in the upper plenum. A higher quality existed than was predicted.

Comparisons of the RELAP4 predictions with the corresponding volumetric flow rates measured by the fuel rod shroud upper and lower turbine meters for Rod 312-2 are shown in Figures 12 and 13. For the most part, both the data and predictions for the other test rods follow the trends shown for rod 312-2. With the initiation of blowdown, the check valves shut instantaneously with the differential pressure reversal. Thus, as shown in Figure 12, the upper turbine meter indicates a small, initial negative flow spike following the cold leg blowdown, and then stagnant conditions exist for the remainder of the transient in the upper portion of the flow shrouds. The RELAP4 predictions follow the measured data very closely. Figure 13 compares the measured and predicted lower turbine flow rates. With the initial negative flow spike, the turbine meter saturates at -1.5 1/s. Beyond this point, the data indicate significant volumetric flow for the next 2.5 seconds, and then flow stagnation for the duration of the transient.

Figures 14 and 15 show the long-term behavior of the four upper and lower flow turbines. Figure 14 indicates stagnant flow at the upper turbines until 123 seconds, when steam formation from the reflood water that was injected at 120 seconds, generates the volumetric flows shown. At approximately 239 seconds into the transient, the quench system was activated and generated the volumetric flows shown from quench front steam formation.
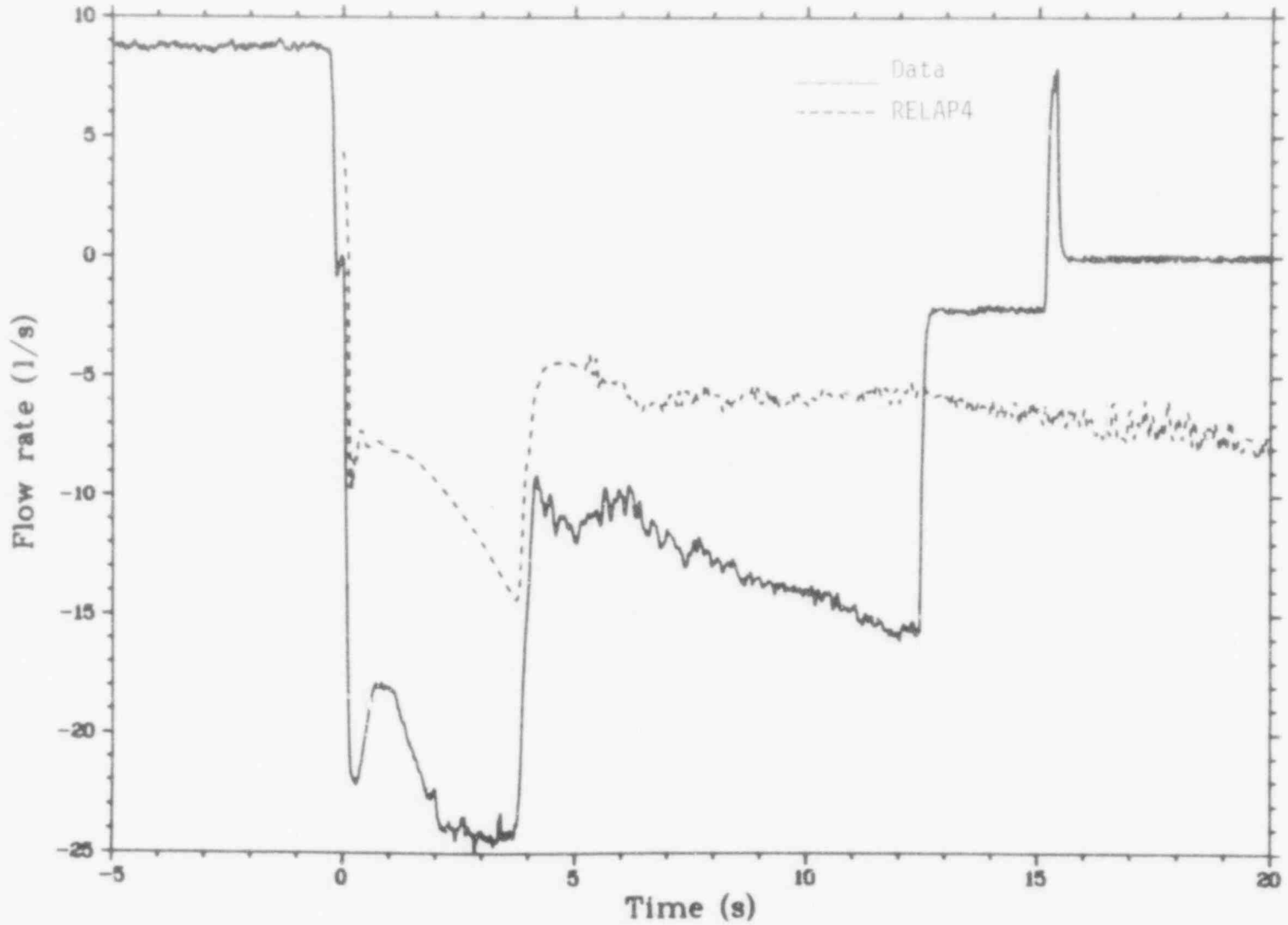
34

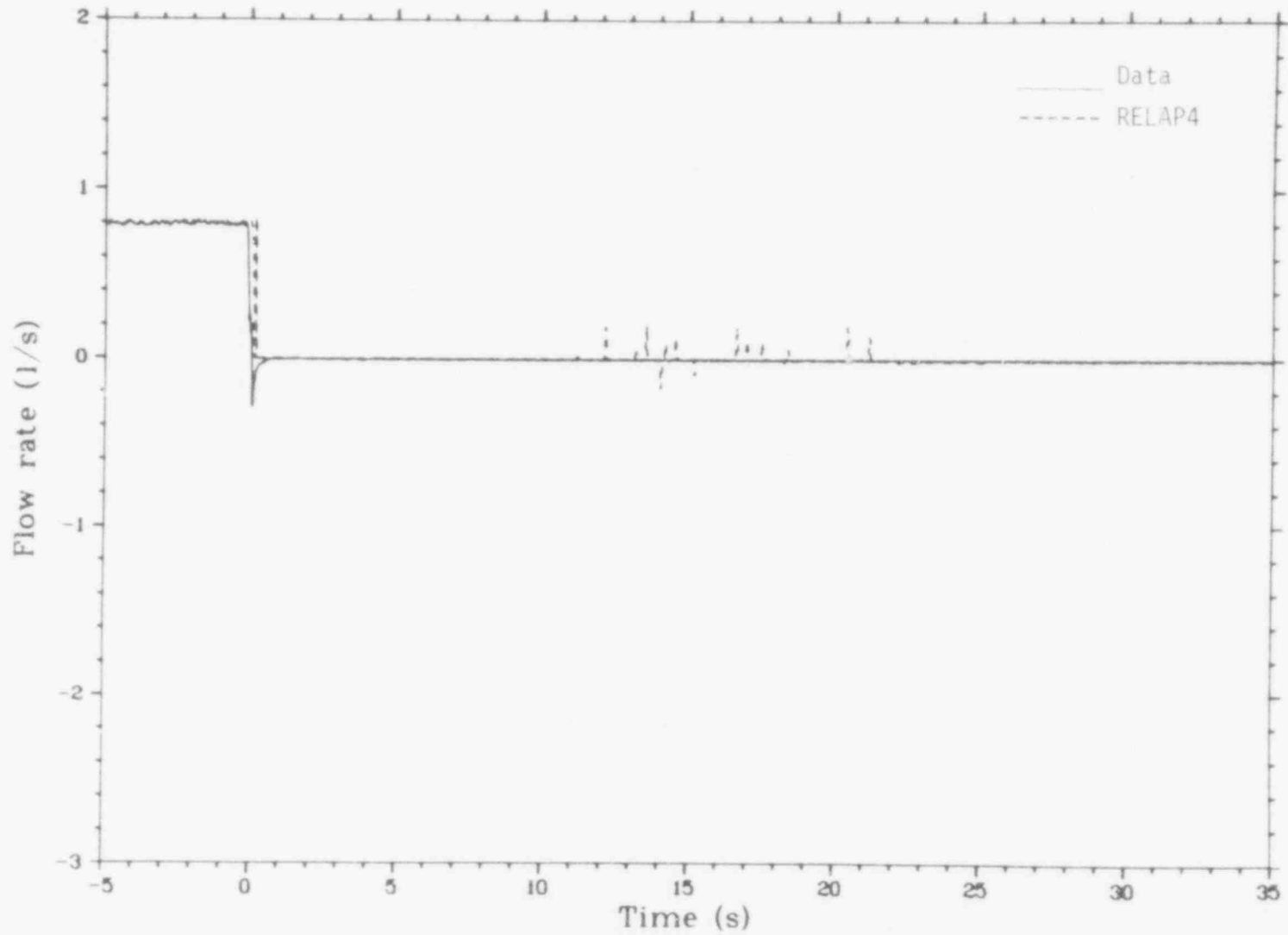Fig. 11 Test LLR-4 comparisons between analytical and experimental cold leg to upper plenum controlled bypass flow rates.

Fig. 12 Test LLR-4A comparisons between analytical and experimental upper turbine flow rates for rod 312-2.
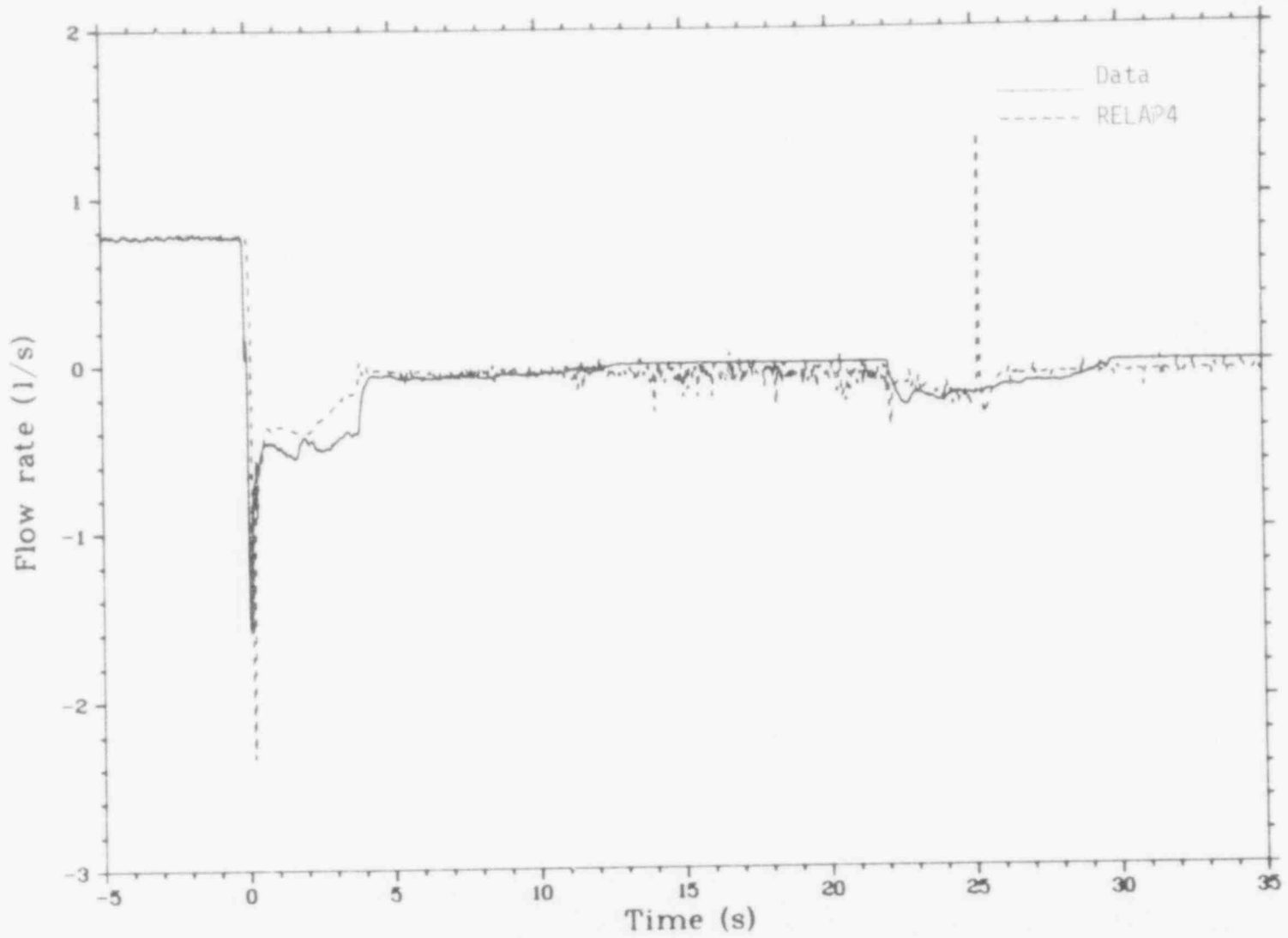
Fig. 13 Test LLR-4A comparisons between analytical and experimental lower turbine
flow rates for rod 312-2.

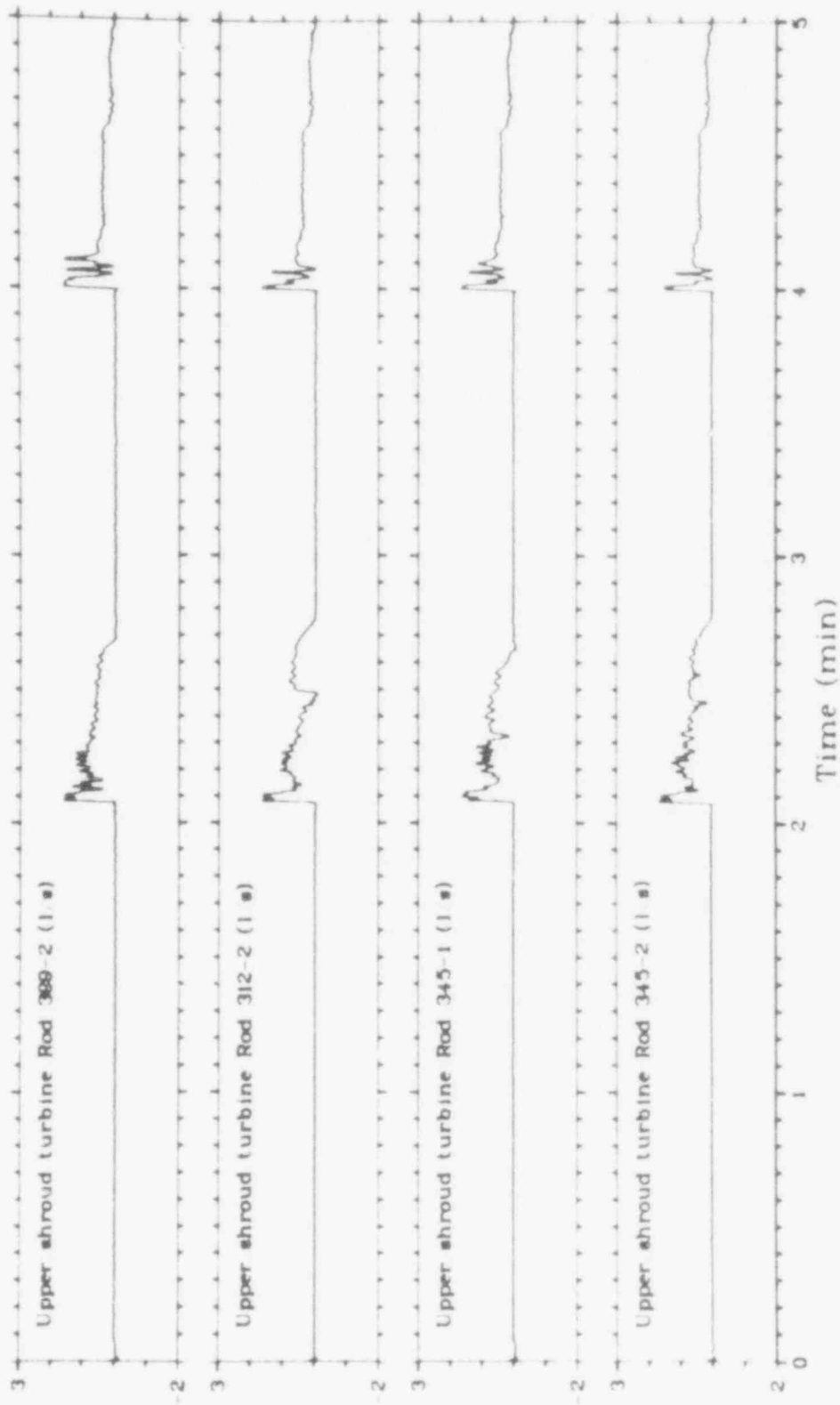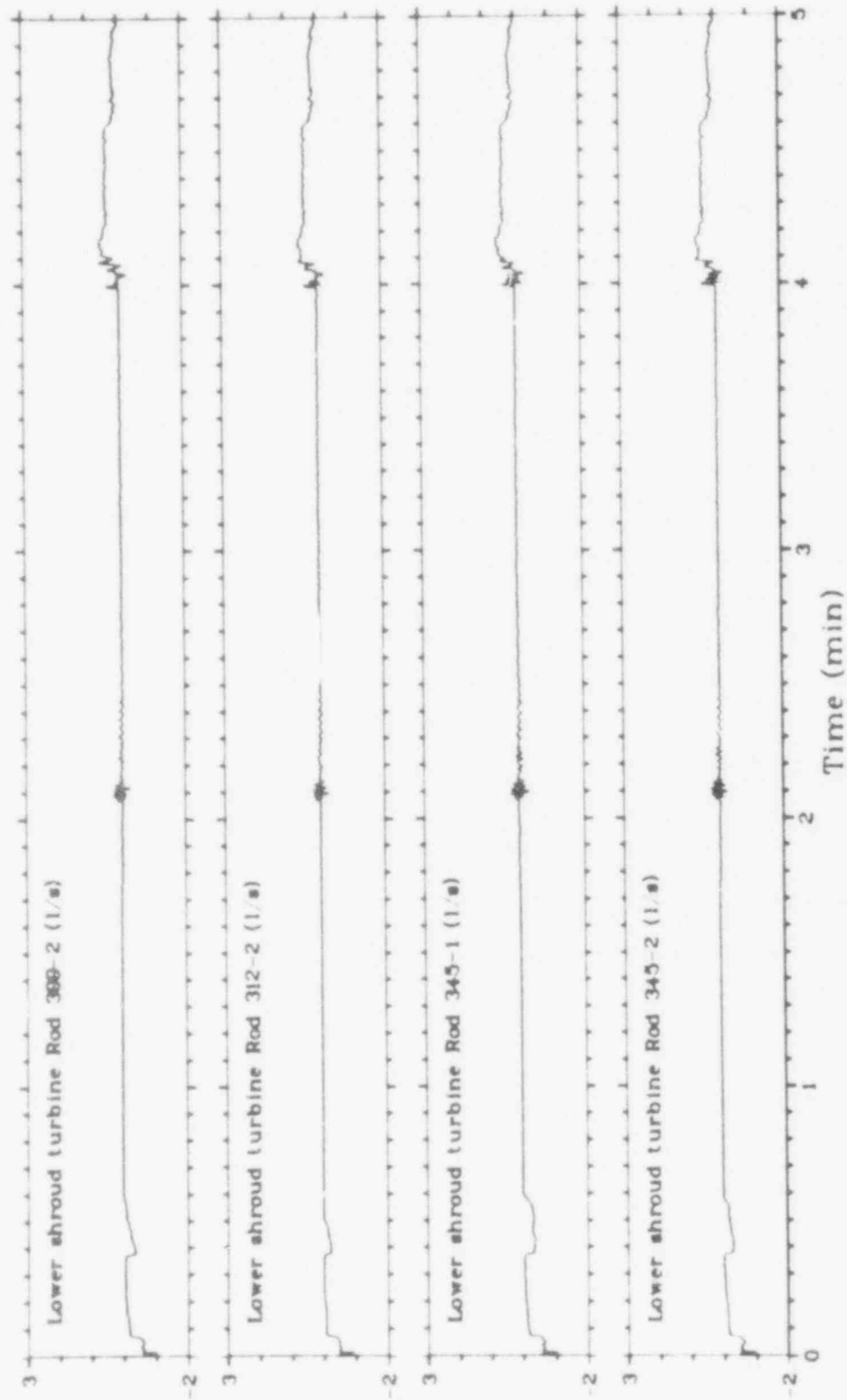Fig. 14 Test LLR-4A experimental upper turbine flow rates for rods 399-2, 312-2, 345-1, and 345-2.

Upper shroud turbine Rod 399-2 (l·s)

Upper shroud turbine Rod 312-2 (l·s)

Upper shroud turbine Rod 345-1 (l·s)

Upper shroud turbine Rod 345-2 (l·s)

Time (min)

480 175

Fig. 15 Test LLR-4A experimental lower turbine flow rates for rods 399-2, 312-2, 345-1, and 345-2.

Figure 15 shows the comparable time response for the four lower turbines. At 22 seconds, the effect of reopening the large cold leg blowdown valve results in a sizeable flow spike on all the rods. Similar behavior as observed on the upper turbines at 123 and 239 seconds was observed on the lower turbines.

4.2 Fuel Rod Behavior for Test LLR-4A

Figures 16 through 26 present the thermal and mechanical behavior for the LLR-4A test fuel rods. Figure 16 presents the cladding temperature and cladding elongation response for rod 399-2 for a 35 second duration. The cladding surface thermocouple data at the 0.314 m 0° azimuthal location indicate the rod achieved DNB at approximately .5 seconds. At 1.6 seconds the rod went into stable film boiling at .314 m. It reached a maximum surface temperature of 1260 K at 8 seconds. The cladding surface thermocouple data at the 0.457 m 180° azimuthal location indicate the rod achieved DNB at the peak power location at 1.8 seconds and a maximum surface temperature of 1205 K at 13 seconds. The centerline thermocouple for this rod failed prior to blowdown. The LVDT first indicated CHF at about 0.25 second and then again at 1.6 seconds. Apparently, CHF began at a relatively low axial position and propagated up the rod during the first 2 seconds of the transient. Figure 17 presents a plot of the rod 399-2 maximum cladding surface temperature versus system pressure and, therefore, the expected mechanical deformation. As shown, based on Olsen's data[12], the cladding was subjected to conditions which would cause cladding waisting. Figure 18 presents the cladding temperature and elongation response for rod 399-2 for a 350 second duration. As shown, good agreement is indicated between the cladding thermocouples and LVDT during the reflood portion of the transient, with quench indicated at approximately 240 seconds into the transient.

The cladding temperature response predicted by RELAP4 is also shown on Figure 16. RELAP4 predicted DNB at about .3 seconds at .3 m and at about 0.5 second at the 0.457 m elevation, slightly after the
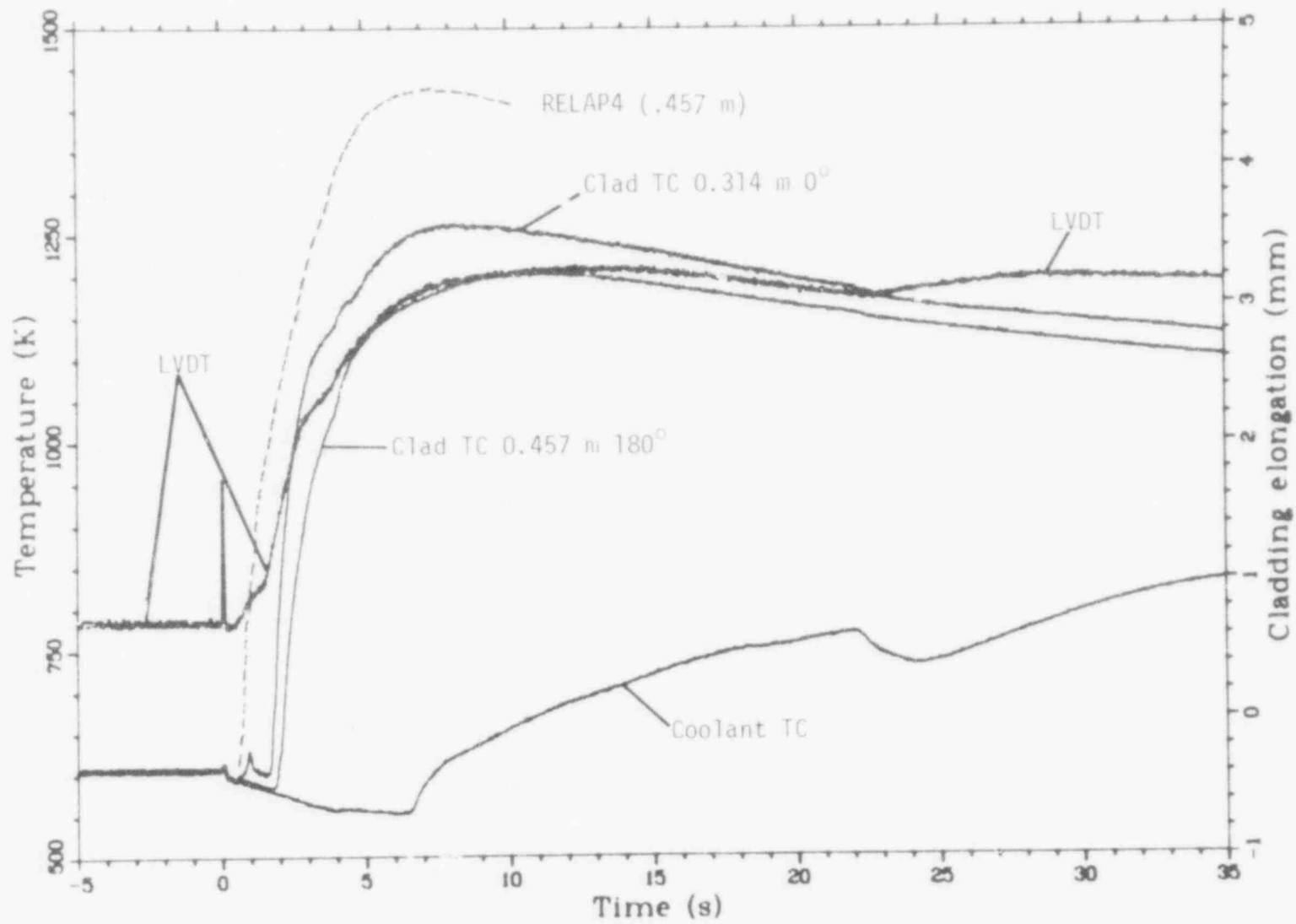
480 177

Fig. 16 Test LLR-4A thermal and mechanical behavior for rod 399-2 (35 second plot).
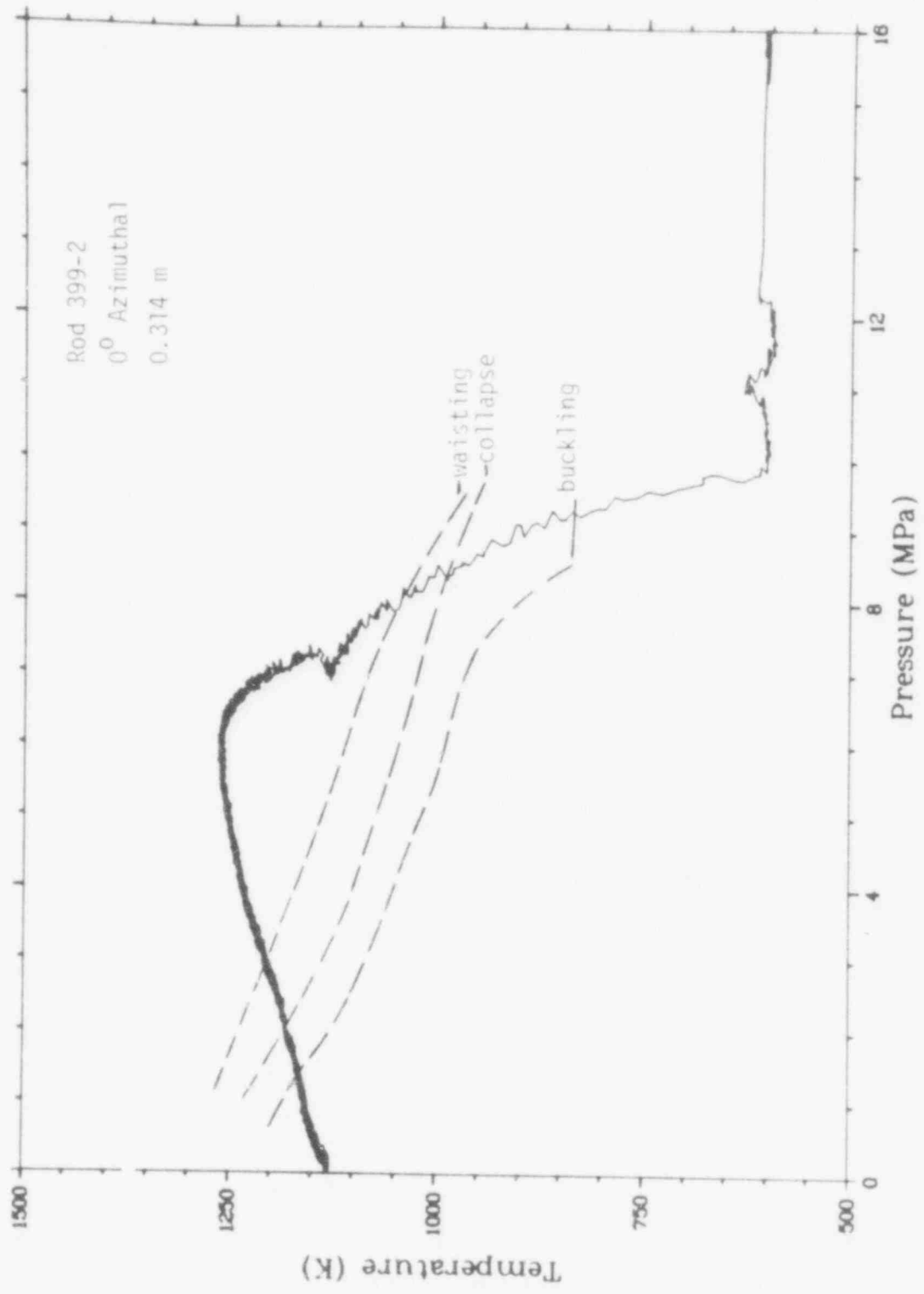
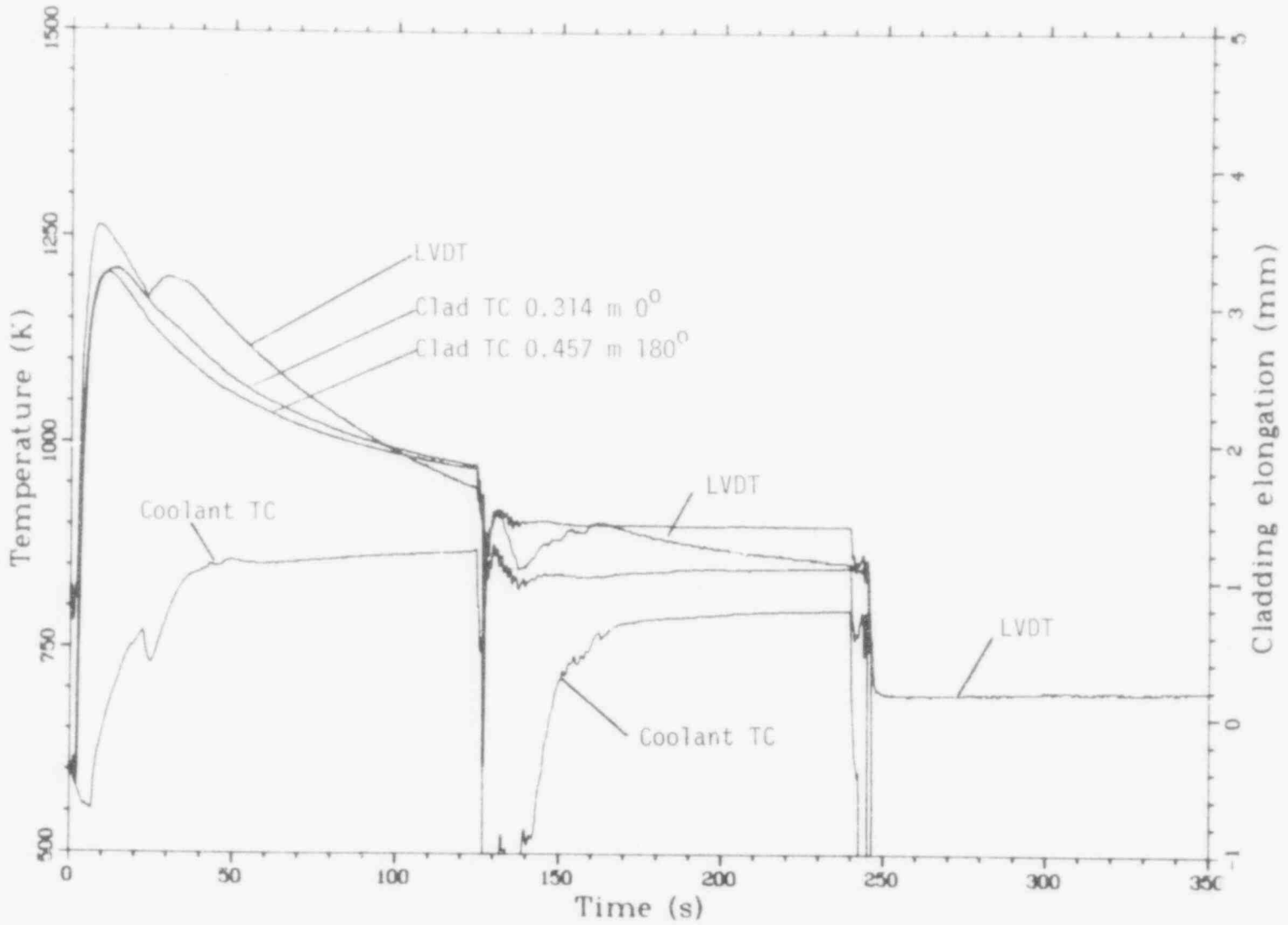Fig. 17 Test LLR-4A rod 399-2 surface temperature versus pressure response.

Fig. 18 Test LLR-4A thermal and mechanical behavior for rod 399-2 (350 second plot).

first indication by the LVDT at 0.25 seconds and well before the thermocouple indication at .457 meters. The peak temperature calculated by RELAP4 was 1435 K at the .457 meter elevation, approximately 200 K above the measured values. RELAP4 predictions are not presented in the remaining temperature plots, however, the discrepancy between measurement and prediction is about the same for the remaining rods as it is for rod 399-2.

Figures 19 through 21 present the cladding temperature and mechanical response for rod 312-2. The cladding temperature data in Figure 19 indicate that the rod achieved DNB at the high power region at approximately 1.8 seconds and reached a maximum hot spot temperature of 1150 K at 6 seconds. As shown in Figure 20, based on Olsen's data, the cladding temperatures reached values required for waisting. The LVDT for this rod failed prior to the transient. Figure 21 represents the long term behavior for the rod cladding temperature. As shown, quench is indicated at approximately 240 seconds into the transient.

Figures 22 through 24 present the thermal and mechanical response for rod 345-1. The cladding surface thermocouple data at the 0.533 m 0^0 azimuthal location show that the rod achieved DNB at 1.8 seconds and a maximum surface temperature of 1075 K at 8 seconds. The LVDT first indicated CHF at about 0.2 seconds, then at 0.4 seconds, and then again at 1.8 seconds when apparently the high power (center) region of the rod went into CHF. This rod exhibited somewhat anomalous behavior in Tests LLR-5 and LLR-4, rewetting at early times before drying out and attaining maximum cladding temperatures. This behavior was attributed to a slight leakage through the Rod 345-1 check valve during the first 4 seconds of the transient in these tests. This check valve was replaced prior to Test LLR-4A, and the new check valve apparently eliminated the rewet condition. The upper and lower turbine meters for this rod exhibited similar flow responses as the other flow shroud turbines during this time period for this test.
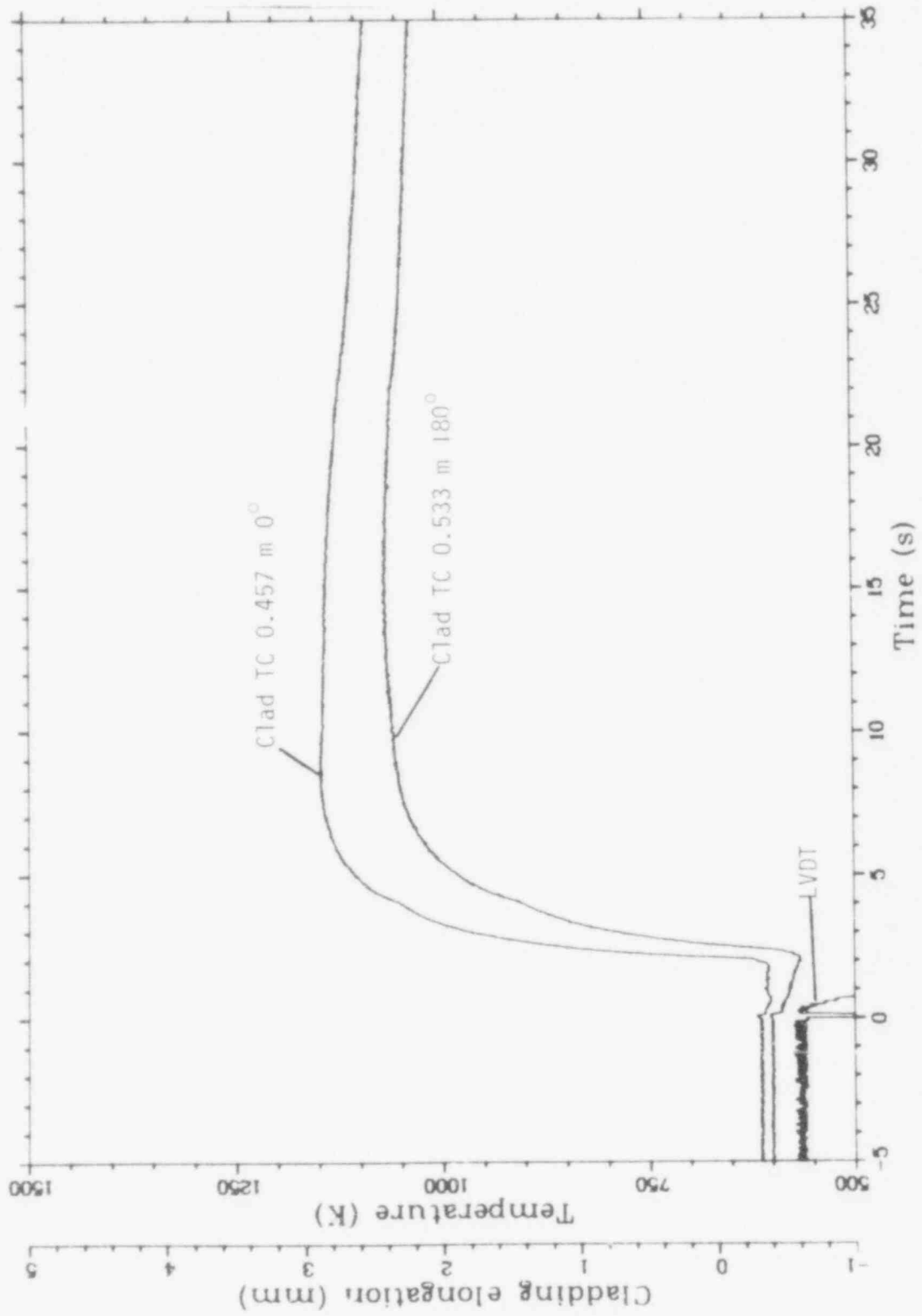
490 181

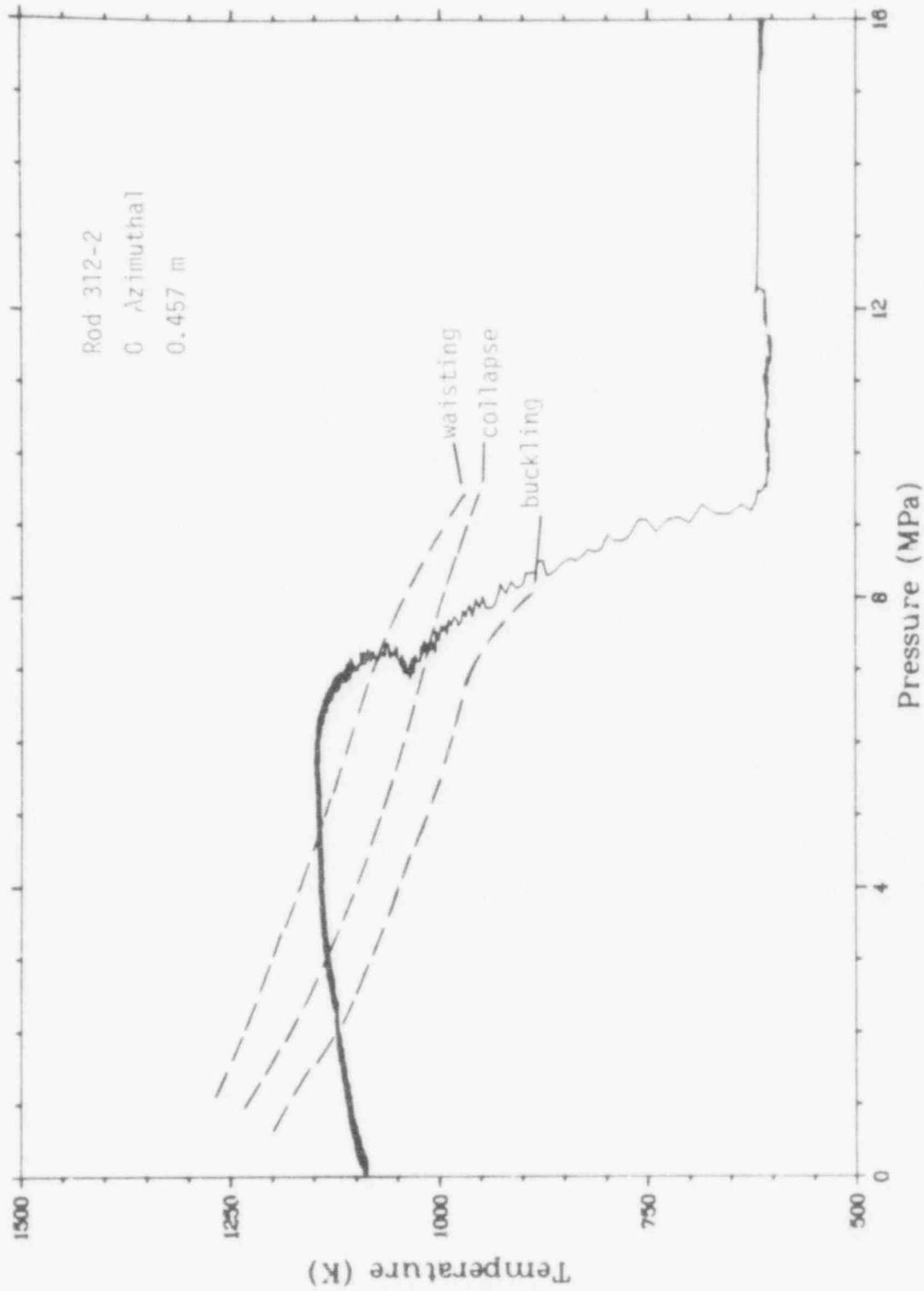Fig. 19 Test LLR-4A thermal and mechanical behavior for rod 312-2 (35 second plot).

Fig. 20 Test LLR-4A rod 312-2 surface temperature versus pressure response.
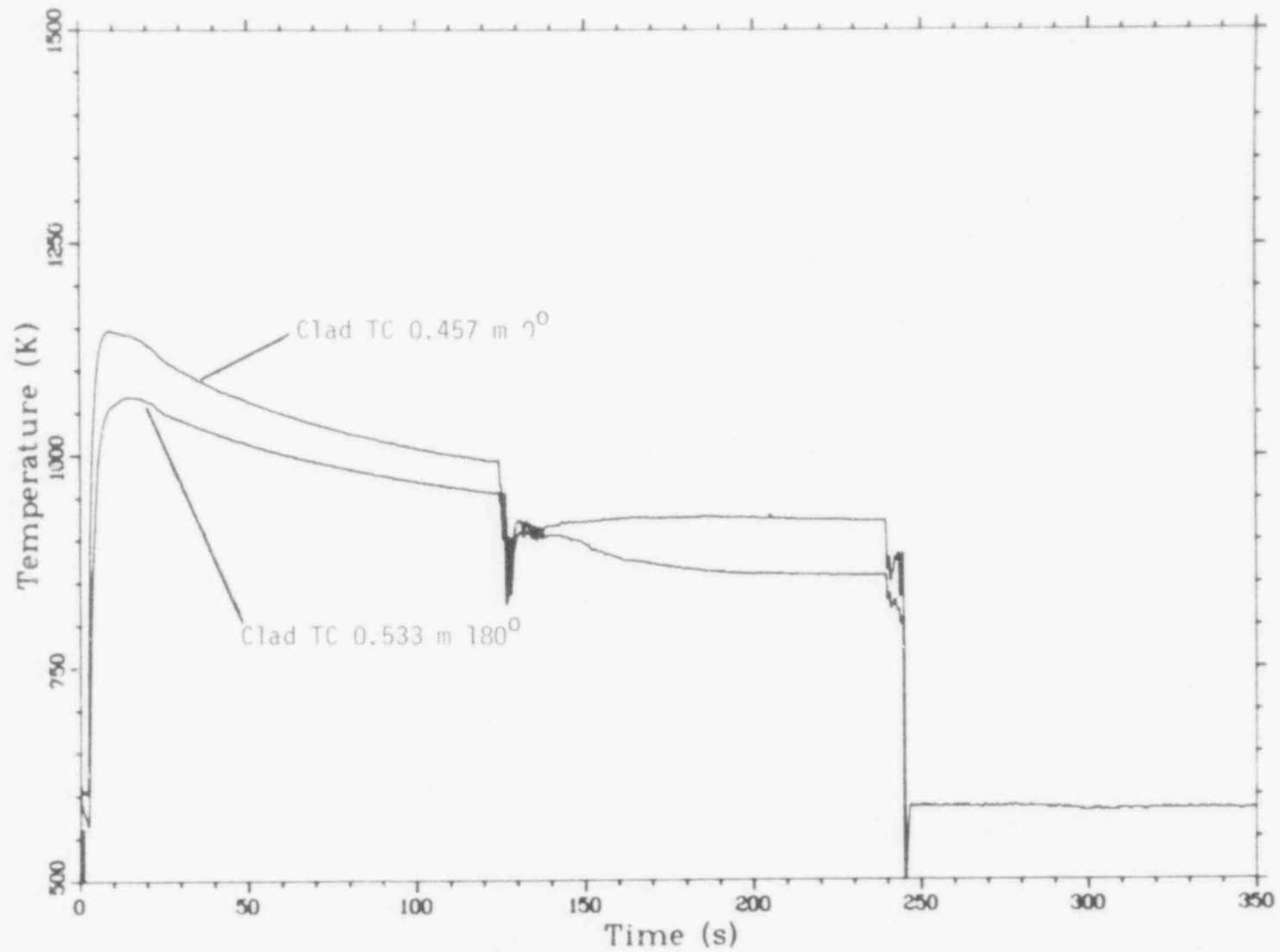
46

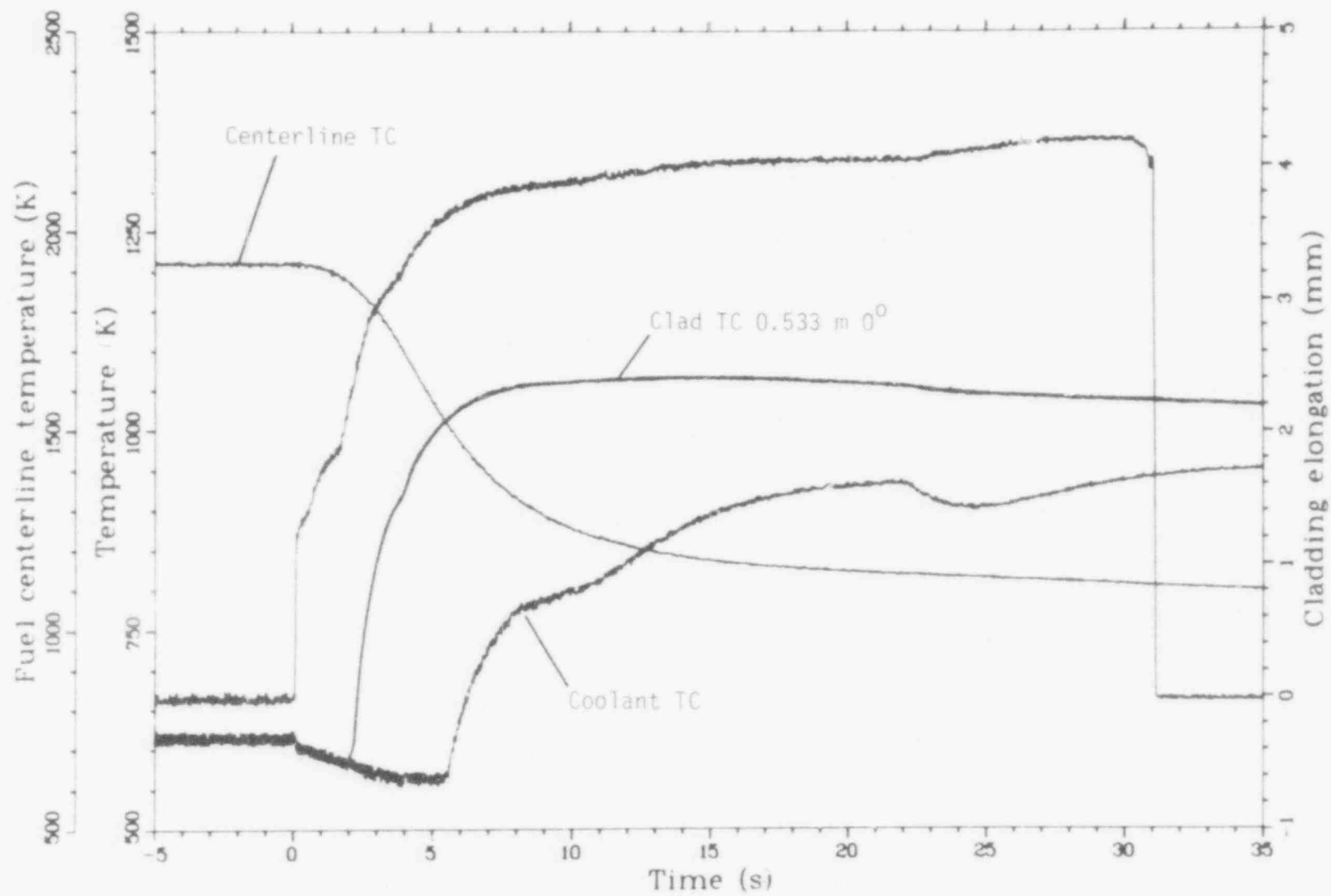Fig. 21   Test LLR-4A thermal and mechanical behavior for rod 312-2 (350 second plot).

Fig. 22   Test LLR-4A thermal and mechanical behavior for rod 345-1 (35 second plot).
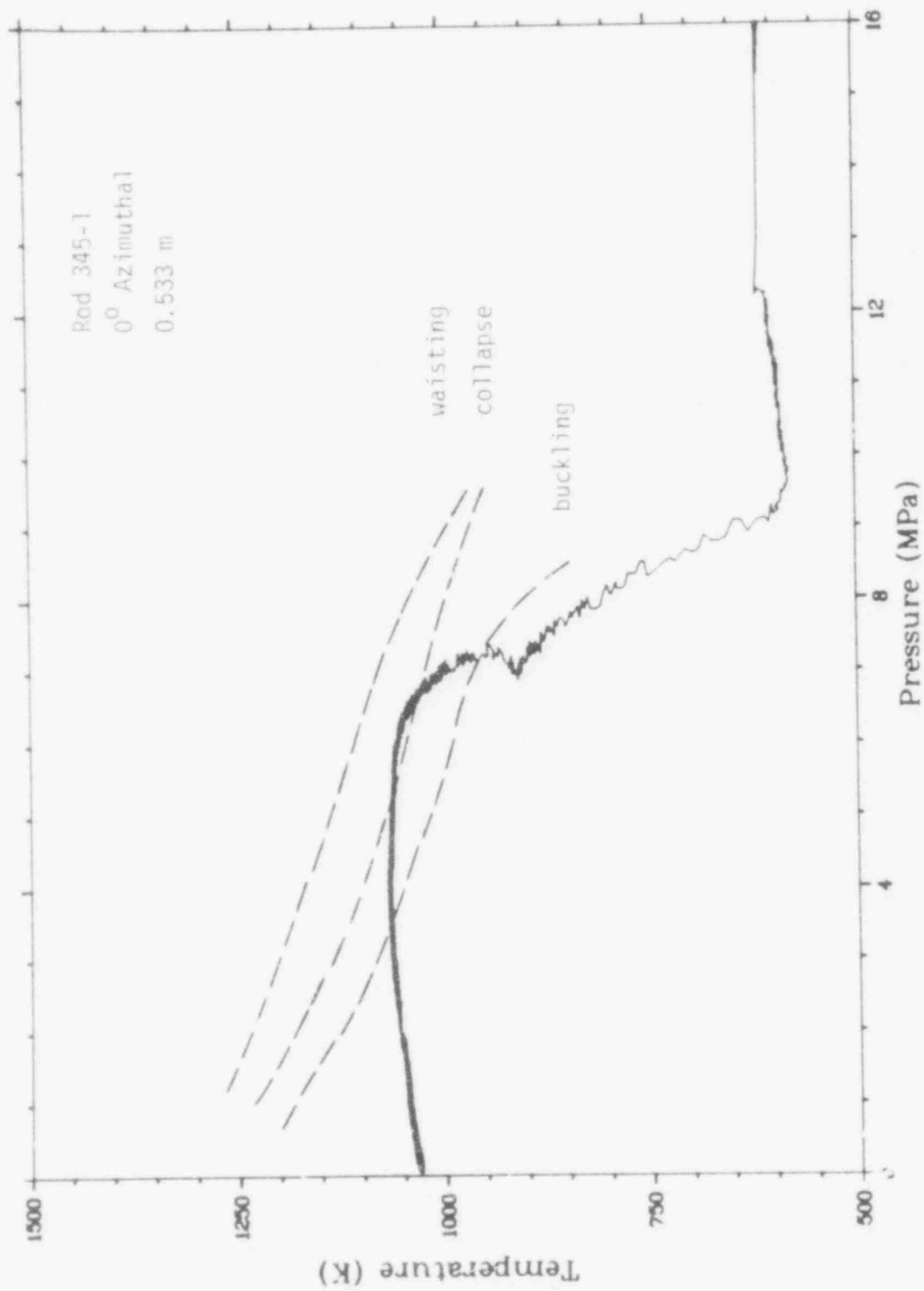
48

Fig. 23 Test LLR-4A rod 345-1 surface temperature versus pressure response.

The Rod 345-1 fuel centerline thermocouple and midplane shroud coolant thermocouple data is also presented in Figure 22. The Rod 345-1 centerline thermocouple indicated a value of approximately 1920 K at steady state conditions just prior to the transient. The FRAP pretest predictions indicated that the steady state centerline temperature for this zircaloy shrouded rod should be about 1770 K at a slightly lower power. The centerline temperature dropped to a value approximately 100 K above the cladding surface temperature within approximately 12 seconds, as expected. The midplane shroud coolant thermocouple response for this rod followed the saturation temperature which corresponded to the system pressure until 5.5 seconds, when superheated coolant conditions within the shroud were indicated for the remainder of the blowdown. Figure 23 presents the mechanical deformation plot for rod 345-1. Based on Olsen's data, uniform circumferential collapse of the zircaloy cladding probably occurred. However, the lower portions of the rod may have been at higher temperatures (as measured on Rod 399-2) and cladding waisting may have occurred below the peak power elevation. As shown in Figure 24, quench occurred at approximately 240 seconds into the transient. The centerline thermocouple lagged the cladding quench time, as indicated by the LVDT, by approximately 5 seconds.

Figures 25 and 26 present the thermal and mechanical response for rod 345-2. The LVDT data show that the rod achieved DNB at about 0.25 seconds. The centerline thermocouple indicated a value of approximately 1865 K at steady state conditions at the 0.457 m location. The LVDT indicated quench at 245 seconds into the transient. The centerline thermocouple response again lagged this quench time by approximately 5 seconds.

4.3 Conclusions for Test LLR-4A

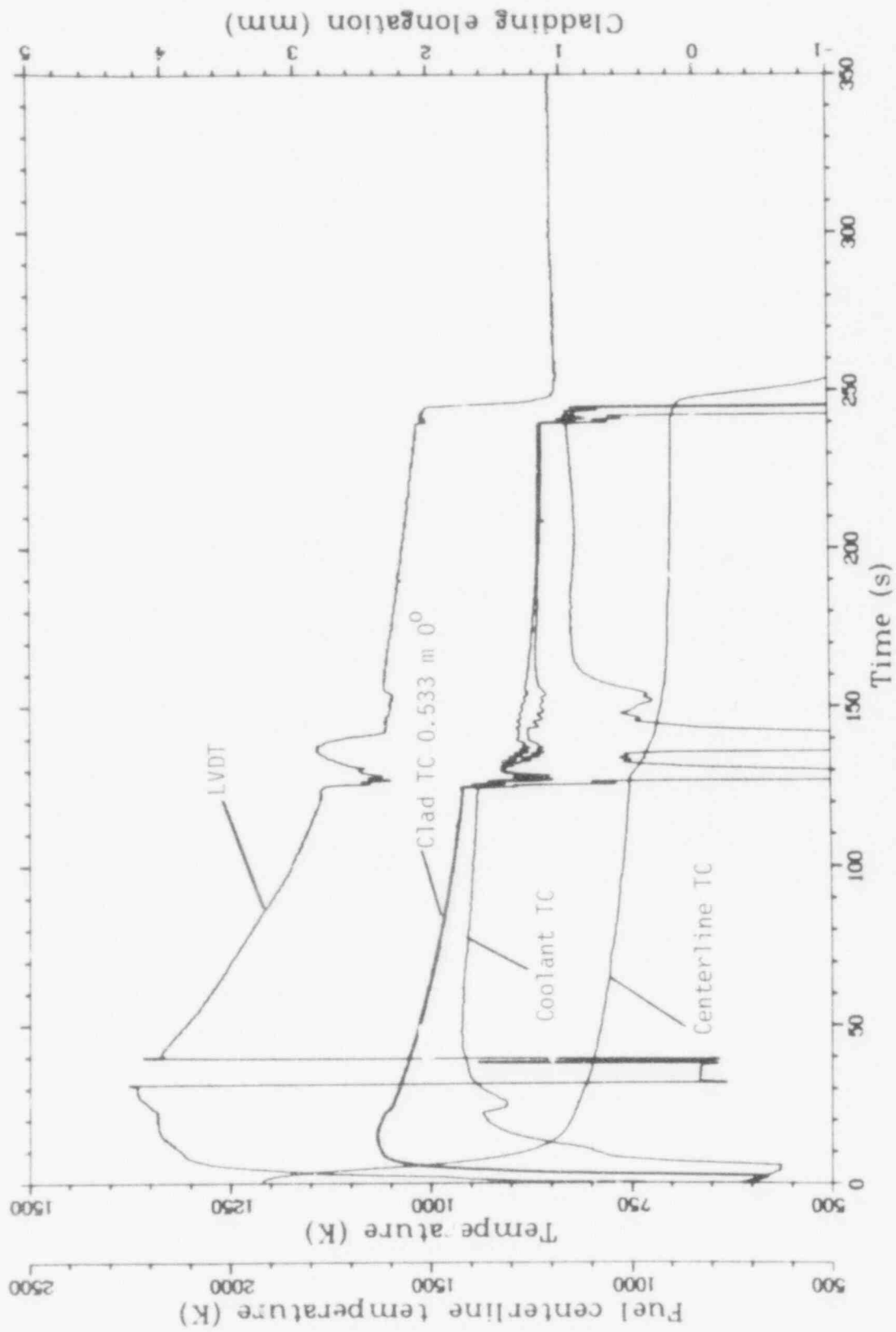The following conclusions are made on the basis of evaluation of the available information.
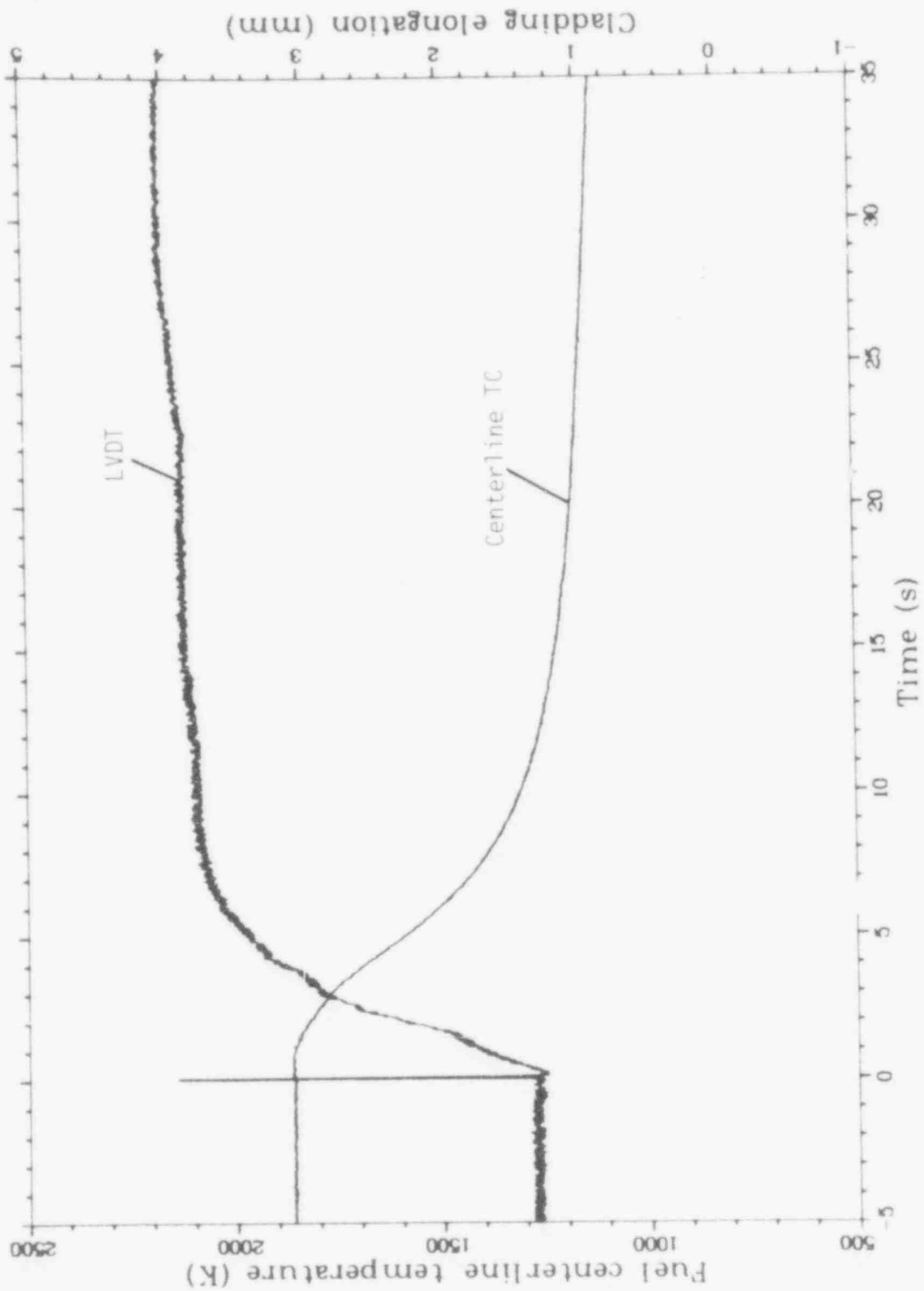
480 187

Fig. 24 Test LLR-4A thermal and mechanical behavior for rod 345-1 (350 second plot).

Fig. 25 Test LLR-4A thermal and mechanical behavior for rod 345-2 (30 second plot).

480 189
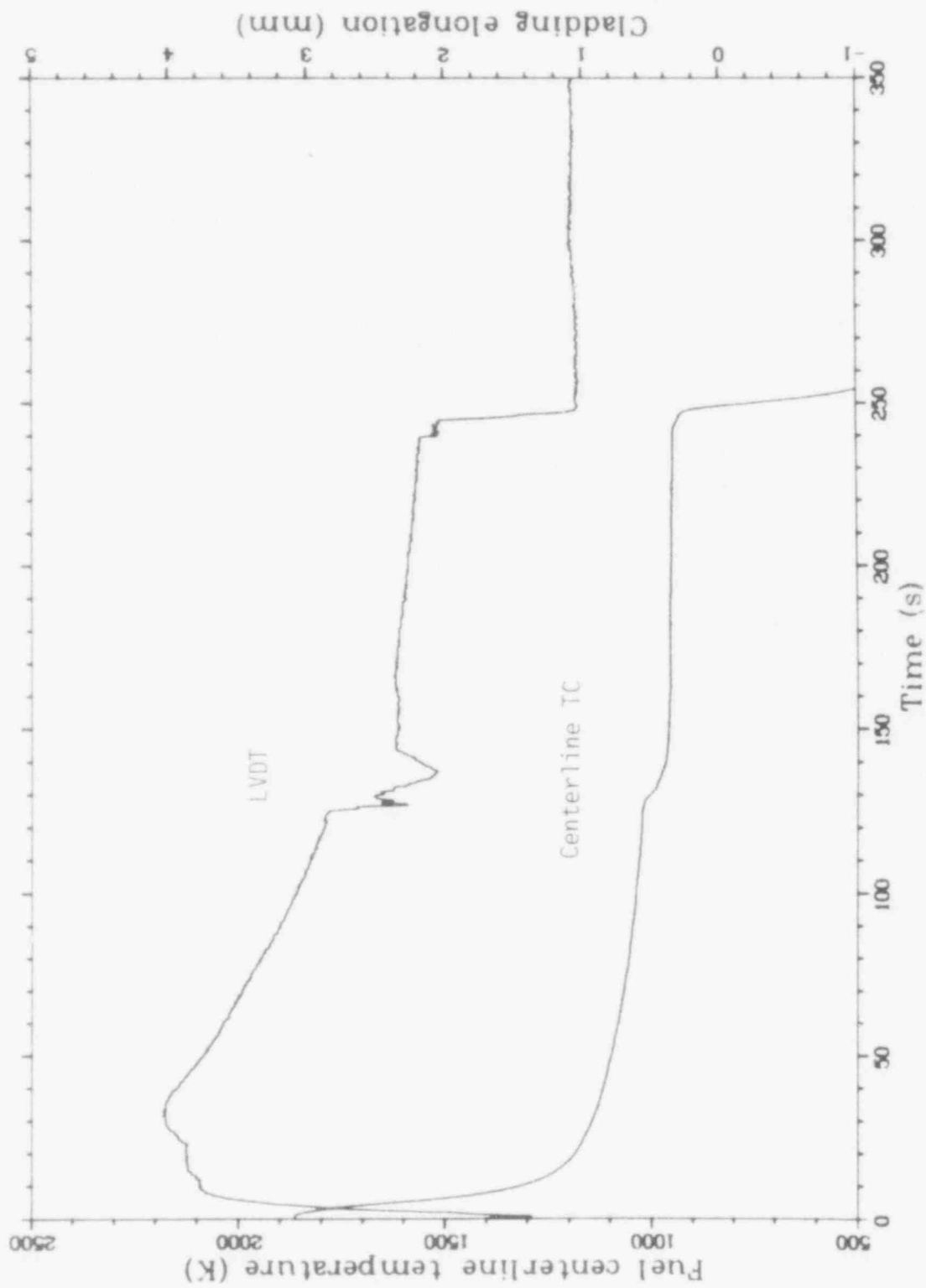
Fig. 2C Test LLR-4A thermal and mechanical behavior for rod 345-2 (350 second plot).

480 190

(1) The test was conducted essentially as planned. An excellent power calibration was achieved during the test. The loop isolation and blowdown valves sequenced properly and the system followed the LOFT required depressurization extremely well.

(2) Each of the four test rods experienced similar thermal-hydraulic boundary conditions throughout the transient. The maximum measured cladding surface temperatures during the transient were: rod 399-2, 1260 K; rod 312-2, 1150 K; rod 345-1, 1075 K. Rod 345-2 was not instrumented with cladding thermocouples. Based on Olsen's[12] data, rods 399-2 and 312-2 experienced cladding waisting. Rod 345-1 experienced uniform circumferential cladding collapse at the peak power location and may have experienced waisting at a slightly lower elevation (based on the thermocouple readings from Rod 399-2).

(3) Higher cladding temperatures were measured (Rod 399-2) at elevations (0.314 m) lower than the hot spot (0.457 m). Time to CHF (1.6 seconds) was faster at this location than at the hot spot (1.8 seconds) as predicted by RELAP4.

(4) The RELAP4 and FRAP pretest predictions of maximum cladding temperature did not agree with the measured values. The RELAP4 pretest predictions of time to CHF at the .3 m elevation were close to the data but the predictions at the peak power elevation did not agree with the data.

(5) The reflood portion of the transient was not successful. Reflood was initiated at 120 seconds; but, the low flow valve did not open at 125 seconds, preventing reflood of the active fuel length.

5. REFERENCES

1. D. J. Varacalle, "PBF/LOFT Rod Test Program Experiment Specification Document", TFBP-TR-282, June 1978.

2. W. P. Polkinghorn, S. B. Letson, "PBF/LOFT Lead Rod Test Experiment Configuration Specification", ES 50364, June 1978.

3. D. J. Varacalle, Jr, "PBF/LOFT Lead Rod Test Program Experiment Operating Specification", TFBP-TR-302, Revision 1, January 1979.

4. LOFT Production Specification, JN-S30061, Revision 4, April 18, 1972.

5. LOFT Production Specification, JN-S30081, Revision 1, March 23, 1972.

6. LOFT Production Specification, JN-S30084, Revision 4, March 23, 1972.

7. L. D. Kirol, "PBF LOCA Blowdown Modification, System Design Description", ANC-70042 Revision A (26 April 1977).

8. K. R. Katsma, et al., "RELAP4/MOD6 - A Computer Program for Transient Thermal Hydraulic Analysis of Nuclear Reactors and Related Systems", User's Manual, CDAP-TR-003 (January 1978).

9. L. J. Siefken, et al., "FRAP-T4-A Computer Code for the Transient Analysis of Oxide Fuel Rods", TFBP-TR-237 EG&G Idaho, Inc., November, 1977.

10. D. J. Varacalle, Jr., et al., "PBF/LOFT Lead Rod Test Program Experiment Predictions Document", TFBP-TR-307, December, 1978.

11. D. J. Varacalle, Jr., R. W. Garner, "PBF/LOFT Lead Rod Program Tests LLR-3, -4, -5 Quick Look Report", TFBP-TR-315, April 1979.

12. C. S. Olsen, "Zircaloy Cladding Collapse Under Off-Normal Temperature and Pressure Conditions", TREE-NUREG-1239, April 1978.

480 192